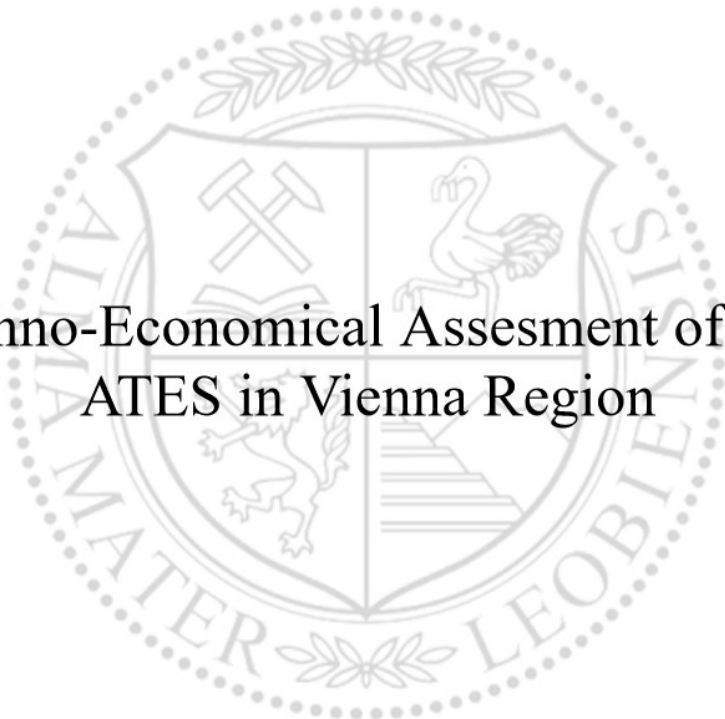




Lehrstuhl für Geoenergy Production Engineering

Masterarbeit



Techno-Economical Assessment of HT-  
ATES in Vienna Region

Josef Studenka, BSc

Februar 2024



**MONTANUNIVERSITÄT LEOBEN**

www.unileoben.ac.at


**EIDESSTATTLICHE ERKLÄRUNG**

Ich erkläre an Eides statt, dass ich diese Arbeit selbstständig verfasst, andere als die angegebenen Quellen und Hilfsmittel nicht benutzt, den Einsatz von generativen Methoden und Modellen der künstlichen Intelligenz vollständig und wahrheitsgetreu ausgewiesen habe, und mich auch sonst keiner unerlaubten Hilfsmittel bedient habe.

Ich erkläre, dass ich den Satzungsteil „Gute wissenschaftliche Praxis“ der Montanuniversität Leoben gelesen, verstanden und befolgt habe.

Weiters erkläre ich, dass die elektronische und gedruckte Version der eingereichten wissenschaftlichen Abschlussarbeit formal und inhaltlich identisch sind.

Datum 02.02.2024

  
\_\_\_\_\_  
Unterschrift Verfasser/in  
Josef Studenka

Josef Studenka

Master Thesis 2023

Industrial Management and Business  
Administration

# Techno-Economical Assessment of HT- ATES in the Vienna Region

Supervisor: Univ.-Prof. PhD Keita Yoshioka

Co-supervisor/Advisor: Dipl. -Ing. Jakob Kulich

Chair of Petroleum and Geothermal Energy  
Recovery

*Janine S.*

*Jannik S.*



## **Acknowledgements**

I extend my sincere gratitude to professor Dr. Keita Yoshioka and co-supervisor Dipl. Ing. Jakob Kulich for their invaluable support and guidance throughout this project.

I would like to express my gratitude to the hatari labs team. Their open-source tutorials have played an important role in advancing my HT-ATES simulation. The wealth of knowledge and resources they provide has had an extraordinary impact on the progress of my work. Thank you for your essential contribution to my project.

# Abstract

High Temperature – Aquifer Thermal Energy Storage (HT-ATES), enables the storage and retrieval of unused or wasted energy during periods of low or representatively high demand. It is presenting a sustainable solution for the currently decarbonizing energy market. Vienna, being the largest city in Austria, has a lot of unused potential when it comes to energy that could be used to heat up water. Moreover, the city already has an established district heating network (DHN). Integrating this storage system within the DHN, would significantly decrease the carbon footprint as the current predominance lies on gas. This work contributes to the limited literature on HT-ATES experiences by presenting a reservoir model established using Modflow, a groundwater-simulating code capable of modelling aquifer systems. Utilizing the graphical user interface, ModelMuse, a simulation is created with varying input parameters. The resulting temperature profile reflects the behaviour of the system forming the foundation for the establishment of the recovery efficiency and the economic variables. Initially, the model was set to a production rate of 3500 m<sup>3</sup>/day, a cut-off temperature (temperature at which the fluid is reinjected back to the reservoir) of 50°C and a reservoir thickness of 50m. During the simulation process, it was of interest to prove the importance of the constantly held thermal radius at 500m, in which the production rate was increased to 4000 m<sup>3</sup>/day. During this scenario, there no breakthrough was encountered, although the produced temperatures were lower compared to the initial production rate. Increasing the reservoir thickness to 75m boosted the recovery efficiency significantly. Even despite the increased thickness, the initial layout, intended for a volume of 3500 m<sup>3</sup>/day showed a higher recovery efficiency than a setup with 4000 m<sup>3</sup>/day. Although the recovery efficiency favours the lower production volume, it does not align with the results of the Levelized Cost of Heat (LCOH) or Net Present Value (NPV). These economic parameters directly benefit from the increase in energy output through the elevated production rate. The evaluation reveals promising outcomes, with the NVP yielding 3,23€ million and LCOH resulting at 55,17€/MWh.

# Zusammenfassung

High Temperature – Aquifer Thermal Energy Storage (HT-ATES) ermöglicht die Speicherung und Rückgewinnung ungenutzter Energie während den Zeiten mit niedriger oder repräsentativ hoher Nachfrage. HT-ATES präsentiert eine nachhaltige Lösung für den derzeitigen Energiemarkt. Wien, als die größte Stadt Österreichs, verfügt über ein großes ungenutztes Potenzial an Energie, das zur Erwärmung von Wasser genutzt werden kann. Darüber hinaus verfügt die Stadt bereits über ein etabliertes Fernwärmenetz. Durch die Integration dieses Speichersystems in das Fernwärme-Netz kann der CO<sub>2</sub>-Fußabdruck erheblich reduziert werden, insbesondere weil das Netz hauptsächlich von Gas betrieben wird. Diese Arbeit soll der begrenzten Erfahrungen mit HT-ATES beitragen, indem sie ein Reservoir-Modell vorstellt, welches mit Modflow erstellt wurde, einem Grundwassersimulationscode, der in der Lage ist, Aquifer-Systeme zu modellieren. Unter der Verwendung einer grafischen Benutzeroberfläche ModelMuse wird eine Simulation mit variablen Eingabeparametern erstellt. Das resultierende Temperaturprofil spiegelt das Verhalten des Systems wider und bildet die Grundlage für die Bestimmung der Rückgewinnungseffizienz und der Wirtschaftlichkeit. Anfangs war das Modell auf eine Produktionsrate von 3500m<sup>3</sup>/Tag, einer Reinjektions-Temperatur von 50°C und einer Reservoir dicke von 50m eingestellt. Während des Simulationsprozesses bestand das Interesse darin, die Wichtigkeit des konstanten thermischen Radius von 500m zu beweisen, bei dem die Produktionsrate auf 4000 m<sup>3</sup>/Tag erhöht wurde. Obwohl es bei diesem Szenario zu keinem Durchbruch kommt, wurden niedrigere Temperaturen produziert. Durch Erhöhen der Mächtigkeit auf 75m konnte die Effizienz signifikant erhöht werden. Das Layout des Models, für welches ein Volumen von 3500m<sup>3</sup>/Tag vorgesehen war, zeigte jedoch trotz der erhöhten Dicke eine höhere Rückgewinnungseffizienz als eine Konfiguration mit 4000m<sup>3</sup>/Tag. Obwohl die Rückgewinnungseffizienz für das geringere Produktionsvolumen spricht, stimmt sie nicht mit den Ergebnissen des Levelized Cost of Heat (LCOH) oder des Net Present Value (NPV) überein. Diese Parameter profitieren direkt von der Steigerung der Energieproduktion durch die erhöhte Produktionsrate. Die Auswertungen zeigen vielversprechende Ergebnisse, wobei der NPV 3,23 Millionen € beträgt und der LCOH bei 55,17 €/MWh liegt

# Table of Contents

Acknowledgements .....	v
Abstract .....	vi
Table of Contents .....	viii
Chapter 1 .....	9
Introduction .....	9
1.1 HT-ATES .....	10
1.1.1 Current known and upcoming HT-ATES projects.....	12
1.2 Geology of Vienna Basin.....	12
Chapter 2.....	15
Methodology.....	15
2.1 HT-ATES Design.....	15
2.2 Capex & Opex.....	18
2.3 Modflow.....	22
Chapter 3.....	25
Results .....	25
3.1 Temperature Profile and Recovery Efficiency.....	25
3.2 The initial model setup (base case) .....	26
3.3 Sensitivity Analysis of LCOH .....	27
3.4 Sensitivity of the modflow inputs .....	28
3.5 LCOH Results.....	32
3.6 Net Present Value .....	34
Chapter 4.....	37
Discussion.....	37
Chapter 5.....	39
Conclusion.....	39
References.....	41

# Chapter 1

## Introduction

Currently, fossil fuels are the primary source of energy in the market, leading to high carbon emissions. This excess CO<sup>2</sup> contributes to the greenhouse effect, causing a rise in the Earth's temperature. To address this issue, 124 countries have committed to attaining carbon neutrality by 2050. This has motivated countries and companies to seek for sustainable methods of powering their industry and homes. (Chen, 2021)

Vienna aims to achieve carbon neutrality by 2040 (Magistratsabteilung 20, 2022). With the new concept 'Wiener Wärme & Kälte 2040', improving and implementing the district heating network (DHN) in new areas will play a key role in the space and water heating industry (Magistratsabteilung 20, 2022). Vienna's energy consumption in 2020 was 40.047 GWh with 88.1% of which was imported. Most of it was natural gas (48%) used for electricity (22%), and DHN (18%) purposes (Figure 23). (Magistratsabteilung 20, 2022) Currently, the district heating network is mainly powered by gas power to heat generation and combustible waste (Stadt\_Wien\_Energiebericht\_2022). The grid temperature is divided into primary and secondary, with maximum temperatures of 160°C and 63-90°C respectively. The secondary network can then directly provide heating or warm water for households (Wien Energie, 2023).

In the future, the High-Temperature Aquifer Thermal Storage (HT-ATES) method could replace current ways of energy storage in Vienna, which would also impact the energy distribution for DHN. Additionally, the waste heat produced by various industries in the city could be utilised for this process. The supply, demand and coverage of waste heat have been studied by (Loibl et al., 2017). The following Figure 1 depicts the distribution of areas with potential waste heat in Vienna. Up to 500GWh could be additionally used for the DHN or seasonally stored (Loibl et al., 2017).

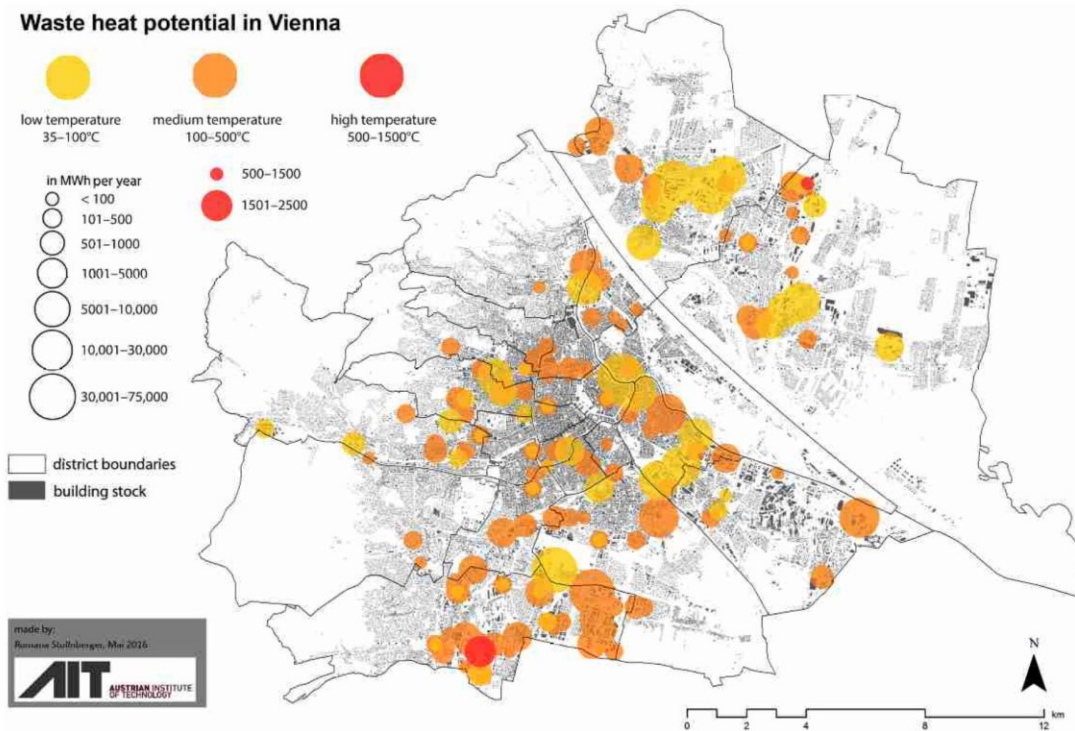


Figure 1: The potential waste heat distribution in Vienna. (Loibl et al., 2017, p. 10)

## 1.1 HT-ATES

Aquifer thermal energy storage (ATES) is a form of underground thermal energy storage (UTES). It employs an open-loop geothermal system that uses a naturally occurring aquifer to store hot or cold water. Because of its scalability, it is ideal for large-scale applications and can also meet seasonal energy demands. (Fleuchaus et al., 2018; Mindel and Driesner, 2020)

HT-ATES (>45°C) (Bloemendal and Hartog, 2018) systems have a limited global presence, but they offer several advantages over low-temperature ATES (LT-ATES). For instance, they consume less electricity since there is no need for heat pumps. Additionally, depending on the temperature, they can be utilized directly for heating purposes.

Both LT and HT systems consist at least out of one or more wells. The seasonal production can then be determined by the pumping direction (Figure 2). (Fleuchaus et al., 2021)

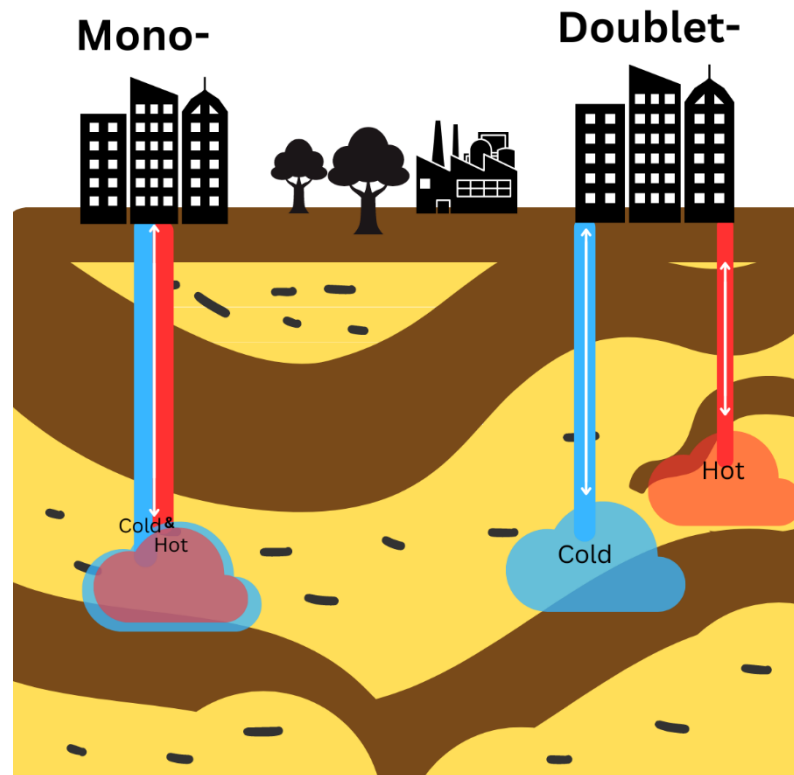


*Figure 2 ATEs-Mono and Doublet-System*

In the double well system cold water is extracted from the reservoir (COLD well) during the summer period (Figure 2, left), which is then heated up to the desired storage temperature. This water is then injected through the HOT well. With the increasing energy demand during the winter period, the pumping direction shifts and the production from the HOT well starts. After the heat extraction through a heat pump or DHN, it is reinjected into the COLD well. The cycle starts again after the cold period. The mono well setup is depicted in the (Figure 2, right), in this case the injection and extraction happens through one well.

In the literature there are currently only a few cases for application of HT-ATES systems in cities or larger buildings. And even fewer of those are considering the economic aspect and its profitability.

To make this heating system more appealing to potential investors, it would be beneficial to provide a comparative scale with other heating options such as gas and electricity. This information can help investors make informed decisions and see the advantages of investing in this HT-ATES system.

This can be simply done by implementing the levelized cost of heat (LCOH) calculation, which is based on the methodology of levelized cost of energy (LCOE) coming from the electrical power sector. This formulation has been developed by (Yoann Louvet et al., 2017) for solar thermal energy, but can be used also for other conventional sources of heat.

### 1.1.1 Current known and upcoming HT-ATES projects

The following table was updated to writers' knowledge. Some data might already be out of date, as most of these projects are under development.

*Table 1 Current known and upcoming HT-ATES Projects*

<b>Name/Location</b>	<b>Size</b>	<b>Depth</b>	<b>Temperature</b>
ATES Vienna (FFG Projektdatenbank, 2023)	10 Gwh	-	90C
Geneva	<50 Gwh	500-1100m	34C – Unknown
Bern (Heatstore, 2021)	7-10 MWth	500m	max 120C
Lüdenburg (Fleuchaus et al., 2021)	-	400m	90C
Hamburg (Fleuchaus et al., 2021)	-	-	-
Middenmeer (Godschalk and Oerlemans, 2021)	28 Gwh	400m	85C
Deepstor (Karlsruhe Institute of Technology, 2023)	5 Gwh	1200-1400m	< 170C
TU Delft (Tess Wegman, 2017)	28 Gwh	500m	70C
Berlin (Fleuchaus et al., 2021)	-	320m	70C

## 1.2 Geology of Vienna Basin

The geology of Vienna Basin is very rich in various formations and its complexity; thus, the focus will be only on the geothermal-economically interesting areas.

For this techno-economical assessment, only the south region of Vienna will be reviewed.

The geology of the area close to Vienna is part of the Vienna basin, which consists of various sedimentary formations. From oil and gas projects, Badenium is known to consist of possible sandstone layers with good permeability. The theoretical aquifer in this study is represented by such (Harzhauser et al., 2020; MATHias Harzhauser and Werner E. Piller, 2005; Wessely and



Draxler, 2006) Following figures have been taken from the Geologische Bundesanstalt (GBA) database which can be accessed under: (GBA MapViewer, 2017).

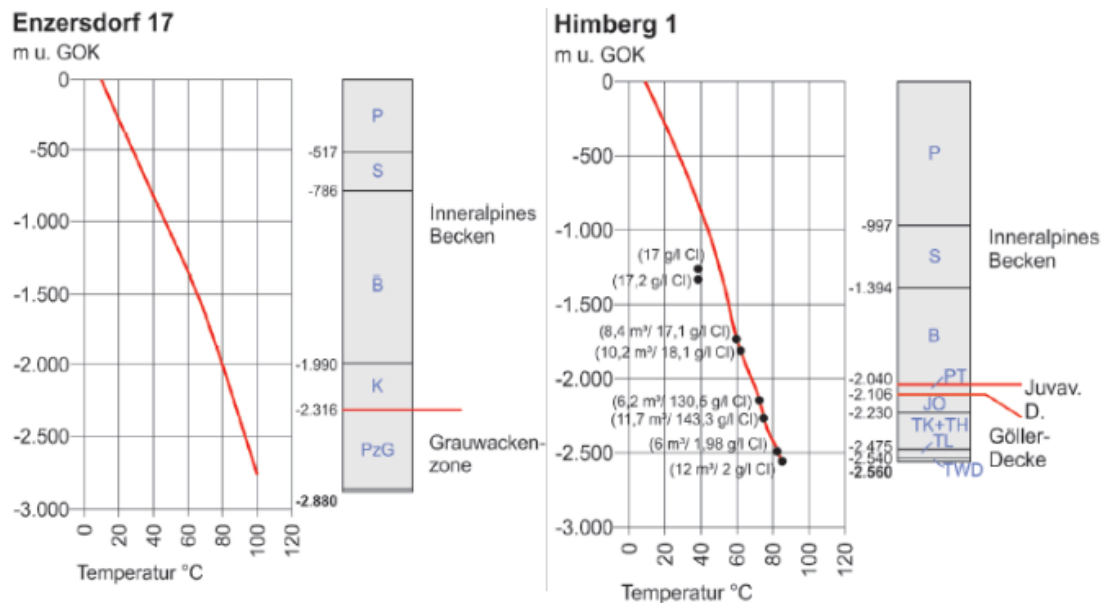


Figure 3 Temperature profile of the Wells: Enzersdorf 17 and Himberg 1 (Geologische Bundesanstalt, 2015)

Comparing the data provided from Figure 3, the area south of Vienna consist of temperature gradients between 3,2 and 3,7 C°/100m. In the case of Himberg 1 well, salinity values are also provided, although these are not used in the calculations.

The Figure 4 depicts a cross section of the Vienna Basin, starting from north-west to south-east, directly between the wells of Himberg 1 and Enzersdorf 17. The red 1500-meter mark represents the depth at which lies the horizon of interest.

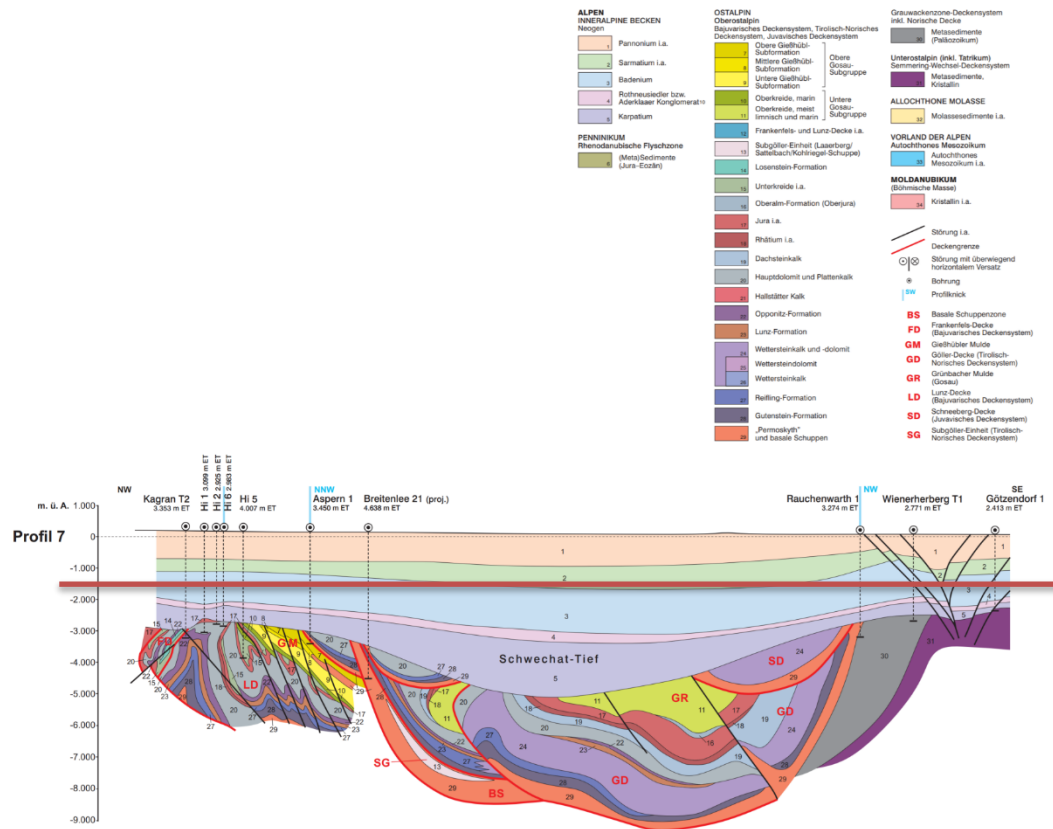


Figure 4 Geological cross section profile from the GBA Database, Autor: Elster et al.

# Chapter 2

## Methodology

Due to the fact that there is only a limited number of studies on the topic considering the economic feasibility of HT-ATES systems across Europe, it is important to incorporate well, site and market specific factors.

The idea of this methodology comes from (Daniilidis et al., 2022). It combines the DH demand of the area, affected by the subsurface properties and the operation CO<sub>2</sub> emissions. The performance of the model is then measured by the capacity, cumulative energy produced and the Levelized Cost of Heat (LCOH).

For this particular case study, it was important that the necessary simulations are done with an open-source model.

The reservoir-model will be done using Modflow. Modflow is a hydrologic model simulating and predicting groundwater conditions and the interactions with surface. (USGS, 2023) Modflow 6 has been chosen due to its versatile and advanced features. In combination with the graphical user interface (GUI) ModelMuse (USGS, 2024) and FloPy (GitHub, 2024; USGS, 2024), which is a Python based package for creating, running and post-processing of modflow-based models, it is possible to create simple and advanced models for the necessary scenario.

The findings illustrate how the injected fluid and temperature diffusion affect the reservoir. The goal is to simulate how efficient the recovery process is and how it changes over the extended lifespan of the system. These results serve as the foundation for the economic model.

### 2.1 HT-ATES Design

During the injection and extraction, the thermal exchange mainly takes place at the outer boundary of the stored body. To simplify the calculations, the shape of the body is considered a cylinder. As a result, the thermal radius can be calculated as followed in Equation 2.1.

$$R_{th} = \sqrt{\frac{c_w * V}{c_a * \pi * L}} \quad 2.1$$

This formula shows that the thermal radius is dependent on the stored volume ( $V$ ), screen length ( $L$ ) (Figure 5), the water and the aquifer heat capacities ( $c_w$ ,  $c_a$ ). The aquifer heating capacity is affected by the porosity ( $\theta$ ) of the reservoir and the heat capacity of the matrix ( $c_{sand}$ ) in following way. (Bloemendal et al., 2018)

$$c_a = \theta * c_w + (1 - \theta) * c_{sand} \quad 2.2$$

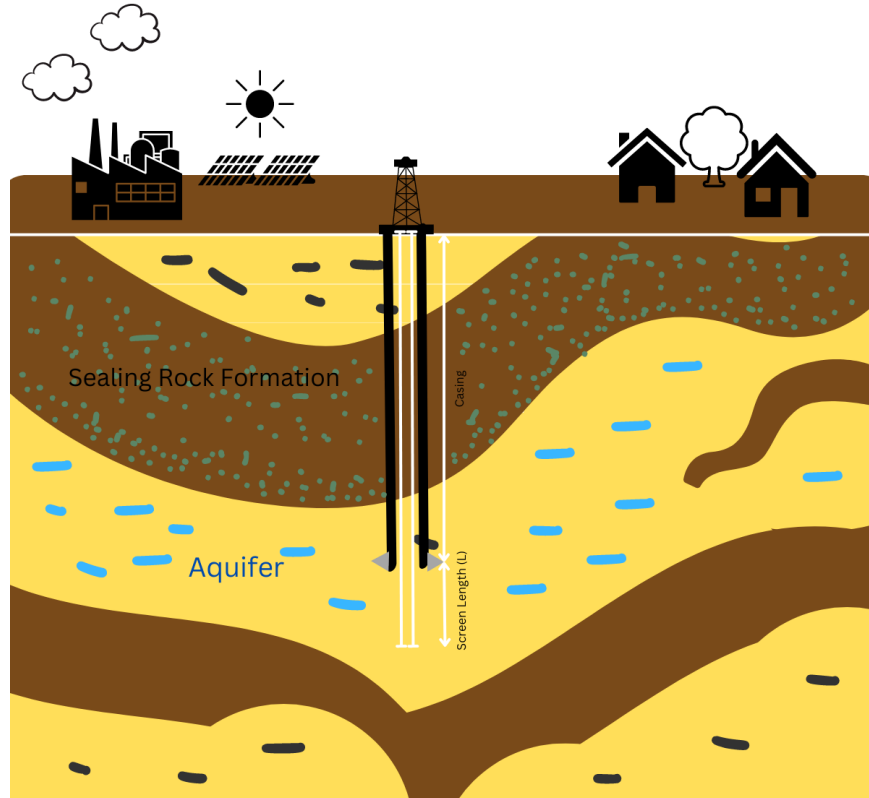


Figure 5 Depiction of the screen length, which represents the open part of the well in the aquifer.

Thermal radius represents the suitable distance between the wells. According to (Bloemendal and Hartog, 2018) the ideal distance between the wells to prevent any interaction between the hot and cold well is three times the thermal radius. Additionally, it should be noted that legal constraints (e.g., by Austrian authorities) might require different regulations.

To get the optimal screen length for a given storage volume, it is essential to identify the point where the conduction and dispersion losses are minimal. This results when the derivate for surface of thermal cylinder is equated to zero. (Bloemendal and Hartog, 2018; Fleuchaus et al., 2021)

$$L = 1.02 \sqrt[3]{V} \quad 2.3$$

Depending on the scenario, the capacity of the system can be either determined by the required volume or by the necessary energy output as depicted in Equation 2.4, where ( $P_{ATES}$ ) represents

the amount of energy, ( $\rho$ ) is the density of water and ( $\Delta T$ ) is the difference between the extracted and injected temperatures (Schüppler et al., 2019). For the base case of this model, a desired yearly volume production was specified and according to it, the necessary pump rate was calculated. For simplification reasons, production and storage time will be set to six months each.

$$V = \frac{P_{ATES}}{c_w * \Delta T * \rho} * 3600 \quad 2.4$$

The required power for the submersible pumps is affected by the depth of the well ( $h$ ), the pumping rate ( $q$ ), the gravity ( $g$ ) and the overall pump efficiency ( $\eta$ ) (Takács, 2018).

$$P_{pump} = q * \rho * g * h * \eta^{-1} \quad 2.5$$

Based on the injected and recovered thermal energy, the recovery efficiency can be calculated as followed:

$$\eta_{th} = \frac{E_{out}}{E_{in}} = \frac{\int \Delta T Q_{out} dt}{\int \Delta T Q_{in} dt} = \frac{\overline{\Delta T}_{out} V_{out}}{\overline{\Delta T}_{in} V_{in}} \quad 2.6$$

The total infused and extracted energy is calculated as the difference between the extracted and injected temperature ( $\Delta T$ ) and the product of cumulated volume ( $V$ ) during that time period.

$$Q_{out} / Q_{in} \quad = \text{well discharge rate}$$

$$\overline{\Delta T}_{out} \quad = \text{weighted average temperature difference for given period}$$

For this case study, volumetric recovery has been seen without any losses which results only in comparison of the temperatures.

Table 2 Input parameters for the technical assessment

	2.3	MED	HIGH	Units	Reference
Depth	-	1500	-	m	-
Density <sub>water</sub>		1000		kg/m <sup>3</sup>	
Specific heat capacity <sub>water</sub>		4184		J/kg/K	
Reservoir Temperature	-	60	-	C	-
Injecting Temperature	-	90	-	C	-

Temperature Cut-Off	40	-	50	C	-
Pump Efficiency	-	60	-	%	(Takács, 2018)
Pumping rate	3500	-	4000	m <sup>3</sup> /day	-
Volume	637000		728000	m <sup>3</sup>	-
Thermal Radius	-	350	-	m	-
Screen Length	50	-	75	m	-
Thickness	50	-	75	m	-
Porosity	-	10	-	%	-
Dispersivity	-	5	-	m	(Dirk Schulze-Makuch, 2005)
Hydraulic Conductivity	-	0.00000222	-	m/s	(Gier et al., 2008; HydroSOLVE, Inc., 2019)
Molecular Diffusion Coefficient	-	6.16*10 <sup>-6</sup>	-	m <sup>2</sup> /s	-
Bulk Density	-	2.6	-	g/cm	
Diffusion Coefficient of the fluid		1.39*10 <sup>-6</sup>		m <sup>2</sup> /s	-

## 2.2 Capex & Opex

The capital and operational expenditures (CAPEX & OPEX) rely on various factors, which are tied to the geographical location of the project and the current economic climate.

One of the main portions of the CAPEX comes from the well drilling cost. The formula used for this case study was adjusted according to various literature reviews, as there is no viable data for the Austrian region, especially for geothermal wells.

The data from Figure 6, compares all those formulas. (Lukawski et al., 2014) presents a paper about a cost analysis for the drilling of oil, gas, and geothermal wells.

- Oil and gas well cost, in millions of U.S. dollars (Lukawski et al., 2014):

$$\text{Well cost} = 1,65 * 10^{-5} * \text{depth}^{1,607} \quad 2.7$$

- Geothermal well cost (Lukawski et al., 2014), using the WellCost Lite model in millions of U.S. dollars:

$$\text{Well cost} = 1,72 * 10^{-7} * \text{depth}^2 + 2,3 * 10^{-3} * \text{depth} - 0,62 \quad 2.8$$

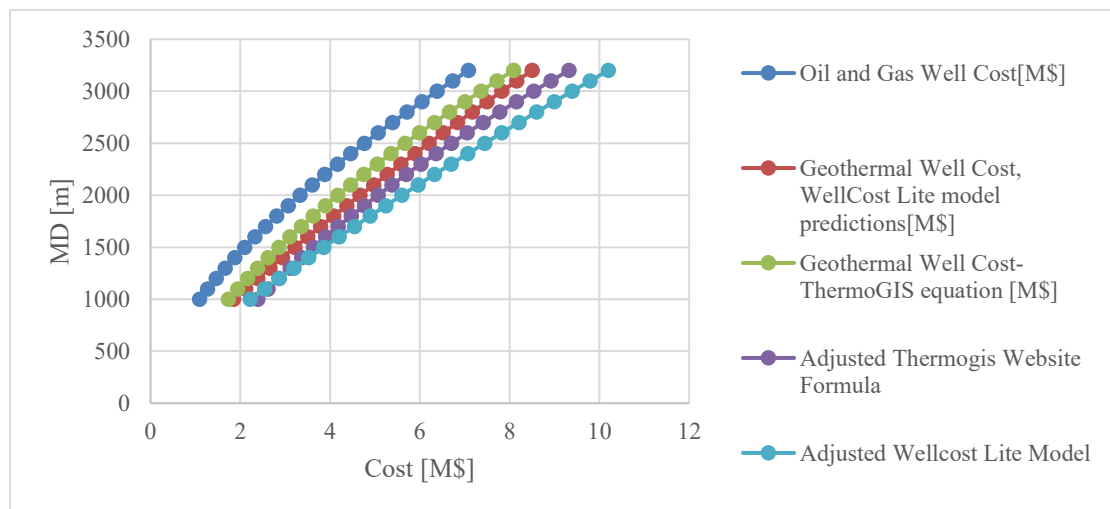


Figure 6 Comparison of drilling-cost formulas from different literature sources. The conversion factor between \$ and € has been kept to the current conversion rate of 1:1.

Additional formula is taken from the Netherlands, which also has been used in the case study for Geneva (Daniilidis et al., 2022)

- Well cost by (ThermoGIS, 2024):

$$\text{Well cost} = 375.000 + 1150 * \text{depth} + 0,3 * \text{depth}^2 \quad 2.9$$

To account for the increasing prices, inflation and escalating costs, the used formulas are adjusted by 35%. The highest yielding result is chosen for the model. For simplification reasons, only two wells will be introduced in this model (HOT & COLD Wells).

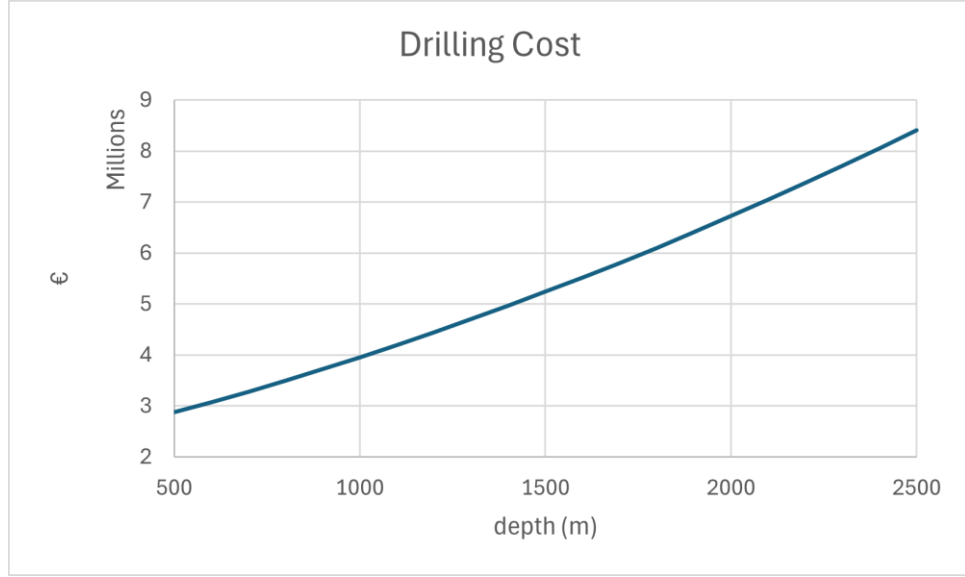


Figure 7 Profile of the adjusted Drilling-Cost Formula.

The total sum for the capital expenditure consists of the drilling cost ( $CAPEX_{drilling}$ ), surface facility ( $Capex_{s.f.}$ ), cost of a heat pump ( $HP_{cost}$ ) and the production pumps ( $ESP_{cost}$ ). As there is no open-source data for the cost of the surface facilities, it was assumed to be 5% of the drilling costs.

$$Capex = n * (Capex_{drilling} + ESP_{cost}) + Capex_{s.f.} + HP_{cost} \quad 2.10$$

The operational expenditures are represented by a percentage from estimated drilling costs, the electricity consumption of the production pumps and their maintenance every 5 years.

$$Opex = Capex_{drilling} * 0,03 \quad 2.11$$

$$+ \sum_{i=1}^n (P_{pump} * el_{price} * working\ time + \frac{ESP_{cost}}{5})$$

The levelized cost of heat is an approach that initially comes from the energy sector, where it is known as LCOE (Levelized Cost of Energy). IEA (International Energy Agency) proposed an easy to use method for calculating the LCOH in Task 54 (IEA SHC || Task 54 || LCoH Tool, 2024) The results can be interpreted as the heat of cost which can be used to compare various heating systems.

$$LCOH = \frac{\sum_{t=0}^n \frac{Capex + Opex}{(1+r)^t}}{\sum_{t=0}^n \frac{E_t}{(1+r)^t}} \quad 2.12$$

Where ( $E_t$ ) represents the total energy extracted during the period ( $t$ ) and ( $r$ ) is the discount rate. With the power of the ATES-System ( $P_{ATES}$ ) calculated as follows, the results being in ( $MWh$ ). (T.M.G. van de Griendt, 2022)



$$P_{ATES} = \frac{q * \rho * c_w * \Delta T}{24 * 3600 * 10^6} \quad 2.13$$

To be able to evaluate the profitability of such a project, the net present value is calculated by discounting the future cash flow ( $CF$ ) to its present value.

$$NPV = \frac{\sum_{i=t}^n CF_t}{(1+r)^t} \quad 2.14$$

*Table 3 Inputs for the economical assessment.*

	Low	Med	High	Units	Source
Heat Pump	-	400.000	-	€	-
ESP	-	400.000	-	€	-
Heat Price	67,07	-	134,141	€/MWh	(Wien Energie, 2024)
Electricity Price	-	0,20	-	€/kWh	(E-Control, 2024)
Drilling Cost (1500m)	-	5.238.000	-	€	-
OPEX-Service	-	32.000	-	€/year	-
OPEX	-	3	-	% of drilling	(Daniilidis et al., 2022)
Wells	-	2	-	n	-
CAPEX surface facility	-	5	-	% of drilling	(Daniilidis et al., 2022)
Discount rate	-	10	-	%	-

These calculations provide a comprehensive understanding of the economic viability and financial sustainability of the system over time.

## 2.3 Modflow

Modflow was chosen for the reservoir simulation as it was possible to simulate heat transport scenarios in the previous versions.

The newest version of Modflow, Modflow 6 (mf6), contains two types of hydrologic models. The groundwater flow (GWF) and groundwater transport (GWT) models. Further than that, mf6 includes packages from other variants like mt3d(Groundwater Solute Transport Simulator) (MT3D-USGS: Groundwater Solute Transport Simulator for MODFLOW | U.S. Geological Survey, 2024) and seawat (Variable-Density Ground-Water Flow and Transport) (SEAWAT: A Computer Program for Simulation of Three-Dimensional Variable-Density Ground-Water Flow and Transport | U.S. Geological Survey, 2024).

The GWF Model for mf6 employs a generalized control-volume finite-difference (CVFD) approach. It is organized into distinct packages, each addressing a specific aspect of the simulation. These packages can be further categorized into those associated with internal calculations, stress packages, and advanced stress packages.

The GWT model for mf6 simulates the three-dimensional transport of a single-solute species in flowing groundwater. Utilizing the CVFD approach, the GWT model employs numerical methods to solve the transport equation. The GWF and GWT models operate simultaneously, portraying a coupled representation of groundwater flow and solute transport. For more detailed information, additional insights can be derived from the provided references.(MODFLOW 6: USGS Modular Hydrologic Model | U.S. Geological Survey, 2024)

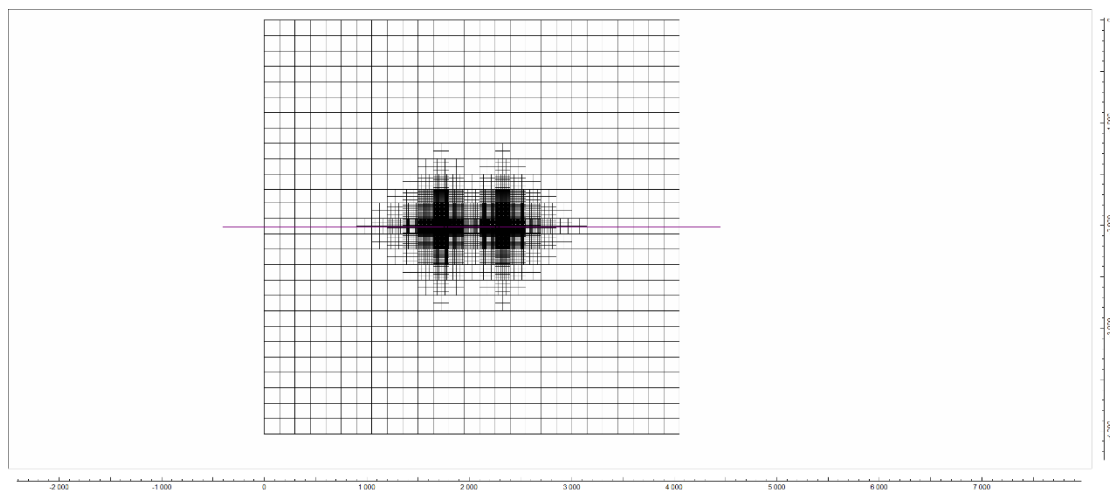


*Figure 8 The initial layout of the modflow model created with ModelMuse. The smallest cells are next to the wells. The distance between the wells is set as 500m due to the calculated thermal radius ( $R_{th}$ )*

The size of the model was determined by the calculated thermal radius of the wells. To ensure that the simulation is not affected by its outer boundary, a grid of sufficient size was created. In mf6, this can be determined by the DIS(Discretization) package.

It is important for the accuracy of the simulation that the cells near the wells are small enough. This results in cells size of approximately 2x2 meters and gradually increasing towards the edge of the grid, with the largest cell being 150x150 meters. Further, it is assumed that the reservoir with a constant thickness is sealed with an impermeable layer from the top and from the bottom, meaning only one layer is necessary. The total size of the grid results in 4000x4000m.

As was already mentioned, the injection and extraction periods are set to 6 months each and the total period of interest is set to 30 years. This can be either directly specified in ModelMuse or with the use of the TDIS-package.

The well settings are carried out using the WEL-package. In which the time-period, pumping rate and an auxiliary variable (concentration, temperature, or others) is used for the setup of the HOT and COLD well.

The initial reservoir conditions are modeled using a general head boundary (GHB-Package). Similarly, the WEL-package requires time-period data and an auxiliary variable, but instead of the pumping rate the head must be specified.

To be able to simulate the ground water transport, additional packages need to be specified.

- BTN: Basic Transport Package
- ADV: Advection Package
- DSP: Dispersion Package
- SSM: Sink and Source Mixing Package
- Solver Package

A newly introduced package in the mt3d-USGS, is the CTS (Contaminant Treatment Package). As in previous simulations, it would be necessary to manually track the changes of concentrations during the time periods, and then transfer this data into the next ones. This package was specifically created to track these dynamic changes, especially for pump-and-treat systems. The pumping-related fluxes are provided from the previously introduced WEL-Package. The total volumetric flow rate in the system is calculated as the sum of all sources in the model and the blended concentration is calculated as the sum of each concentrations ( $C_i$ ) time the flow rate( $Q_i$ ) divided by the total sum of the concentrations ( $Q_{mix}$ ). (Bedekar et al., 2016)

$$C_{mix} = \frac{\sum_{i=0}^n Q_i C_i}{Q_{mix}} + C_{reservoir} \quad 2.15$$

The CTS-Package has four possible settings('treatments') to choose from:

1. Specifying the percent for addition or removal of the selected concentration or mass
2. Adding or removing specified concentration

3. Adding or removing mass
4. Treating up to a specified concentration

For this specific scenario, an ATEs-System, the second treatment option, is chosen. The configuration then clarifies, which well is treated as the injector and which is treated as the extractor. During the injection process a specified concentration is then selected, which is added to the mixture. In this case it is the specified temperature.

It was not possible to import the created model from ModelMuse to the python environment of FloPy, hindering the incorporation of additional packages. Similar case for heat transport simulation is depicted in the seawat guide (C. D. Langevin et al., 2008) The issue described still persists, due to the incompatibility between the CTS-Package from ModelMuse and FloPy, As consequence, the viscosity effect on the transport model was not added and the heat transport simulation was created only with the use of ModelMuse (modflow and mt3d).

In order to simulate the heat conduction during the transport process it is calculated with the following formula:

$$D_{temp} = \frac{k_T}{\theta * \rho * c_{water}} \quad 2.16$$

Due to the mathematical similarity between the molecular diffusion and the thermal conduction, it can be entered into mt3d as the molecular diffusion coefficient. (C. D. Langevin et al., 2008) ( $\theta$ ) represents the porosity and ( $k_T$ ) the thermal conductivity in [W/m/K].

As an addition for monitoring purposes, an OBS (Observation package) is introduced for both Wells. This package delivers a CSV file with the desired output settings.

- Flow observations for the volumetric output [m<sup>3</sup>/day]
- Mass flow observation for the specific temperature of the [C]:

# Chapter 3

## Results

The data for the initial base-case scenario was carefully chosen, adopting the median values from Table 2. A production rate of 3500 m<sup>3</sup>/day and a cut-off temperature of 50°C were deemed optimal for the HT-ATES within the specified area. This selection was done based on the result of discussion between colleagues and the thesis supervisors, aiming to establish the most suitable settings.

With these parameters in place, the simulation spans over a 30-year period with an additional 10 steps per period. The simulation output, extracted from the OBS-CSV, provides a detailed temperature profile crucial for understanding the dynamic behavior of the HT-ATES system over the extended timeframe. This temperature profile sets the groundwork for the evaluation of the system performance, recovery efficiency, and economic metrics in the subsequent sections of this chapter.

The initial sections of the chapter results provide a comprehensive analysis towards the base case scenario. In the subsequent sub-chapter throughout the chapter the base case is expanded by introducing varying variables to explore their impact on the outcomes.

### 3.1 Temperature Profile and Recovery Efficiency

By examining the disparity between the injected and extracted temperatures, the recovery efficiency of the system is determined. The simulation outcomes demonstrate that the recovery efficiency experiences a substantial increase over the lifespan of the system.

The Figure 10 shows that the system's efficiency has grown by from 76,13% to 79,46% over the simulated period. In energy terms, the HT-ATES provides 534MWh more energy at the end of the lifespan than in its first year of use.

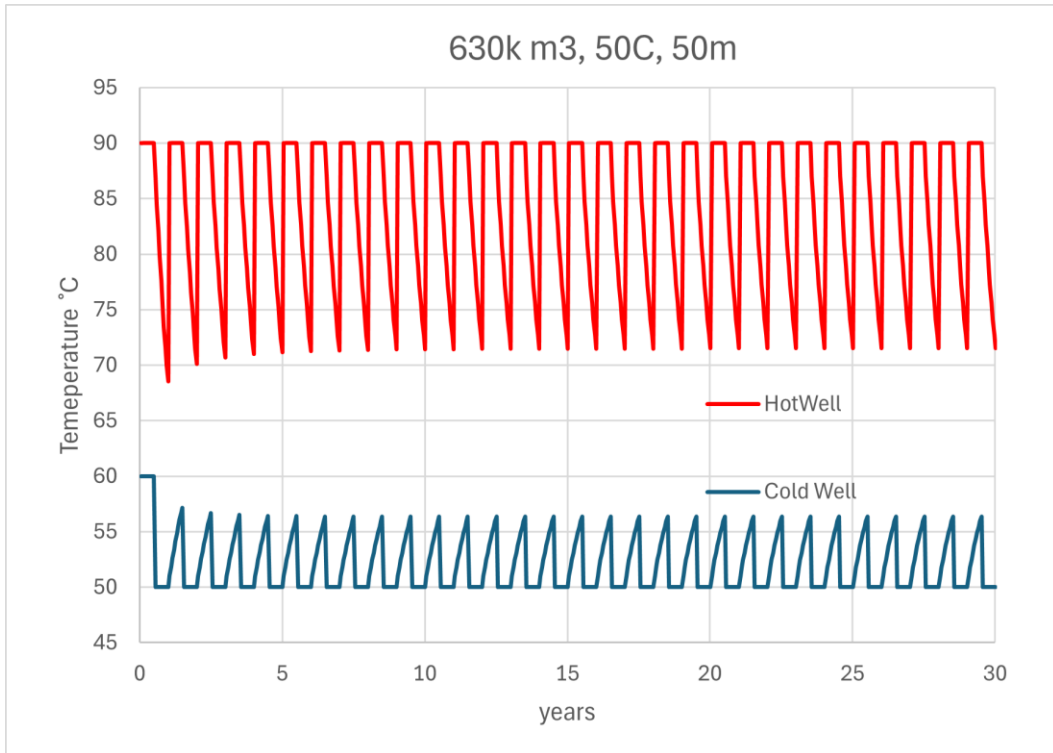


Figure 9 Temperature Profile of the initial modflow setup (3500m3/day, 50m reservoir thickness and 50C cut-off temperature). The blue line represents the production and injection from the hot well, respectively the orange line is the temperature profile of the cold well.

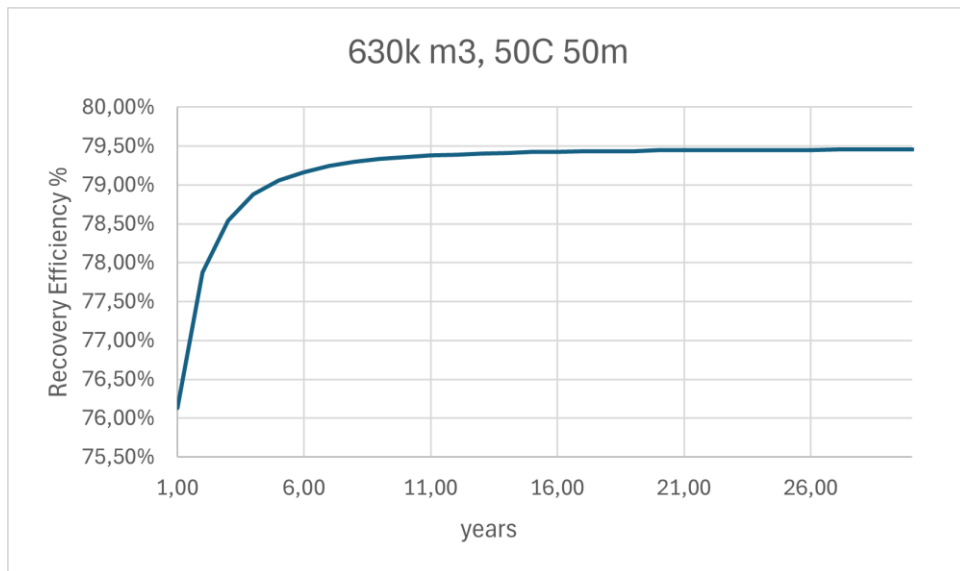


Figure 10 Recovery efficiency of the initial modflow setup (3500m3/day, 50m reservoir thickness and 50C cut-off temperature).

### 3.2 The initial model setup (base case)

Using the attained temperature profile, the energy output of the system is estimated and with the including costs the two crucial financial metrics: Levelized Cost of Heat (LCOH) and Net

Present Value (NPV) are calculated. The initial case assumes that the energy provided for the heating comes at zero cost as it is generated from waste heat. Although in a real-life scenario this might vaguely differ and due to this a comparing scenario is created with the DHN price being discounted by 50%. The initial four years are set for research and development and no revenue or operational expenditures are accounted for.

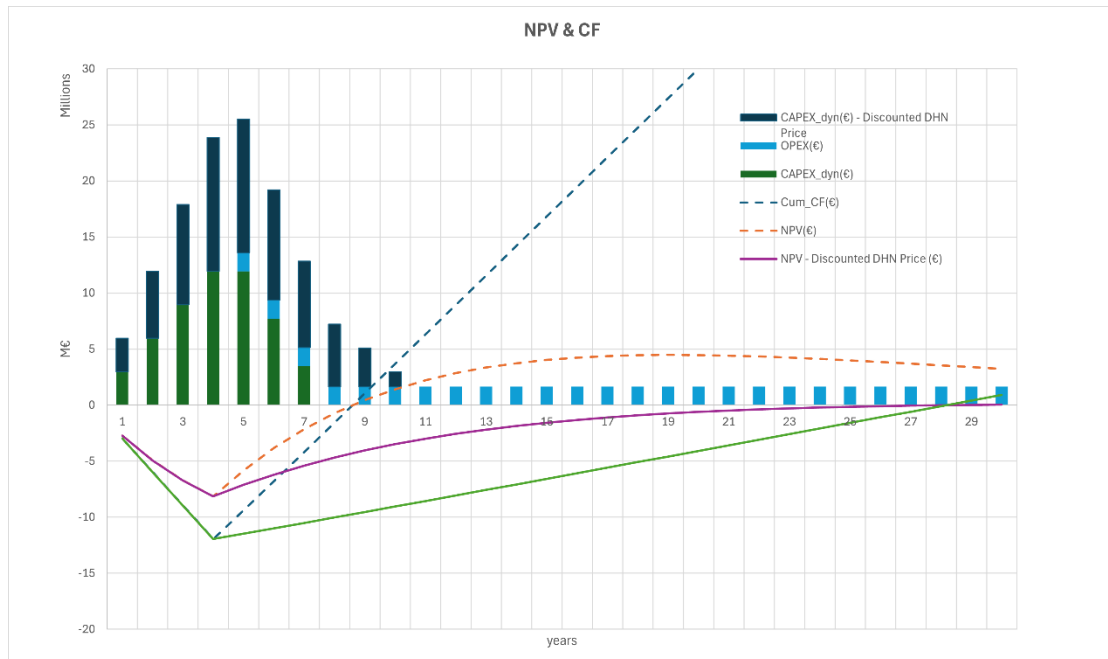


Figure 11 Depicting the difference between the results of cumulative CF and NPV for case 1 and impact of the discounted DHN price.

The resulting NPV and cash flow in (Figure 11), is according to the settings of (case 1), the NPV yields 3,23 million € after the 30-year period. The peak of the NPV is reached after 19 years with it reaching 4,48 million €. Positive cash-flow and NPV are initiated in the 9th year. The capital expenditures are being paid off after the 7th year. Moreover, the discounted DHN price drastically affects the economic feasibility of such project, as the NPV only reaches 0,05 million € at the end of the lifespan and barely experiences a positive cashflow.

### 3.3 Sensitivity Analysis of LCOH

Due to the dynamic nature of the economic market, a sensitivity analysis has been created to simulate the potential impact of various influences on the system. Factors such as capital expenditure (CAPEX), operational expenditure (OPEX), district heating network (DHN) price, and the produced energy by the system are systematically varied to understand their repercussions on the overall economic performance of the system.

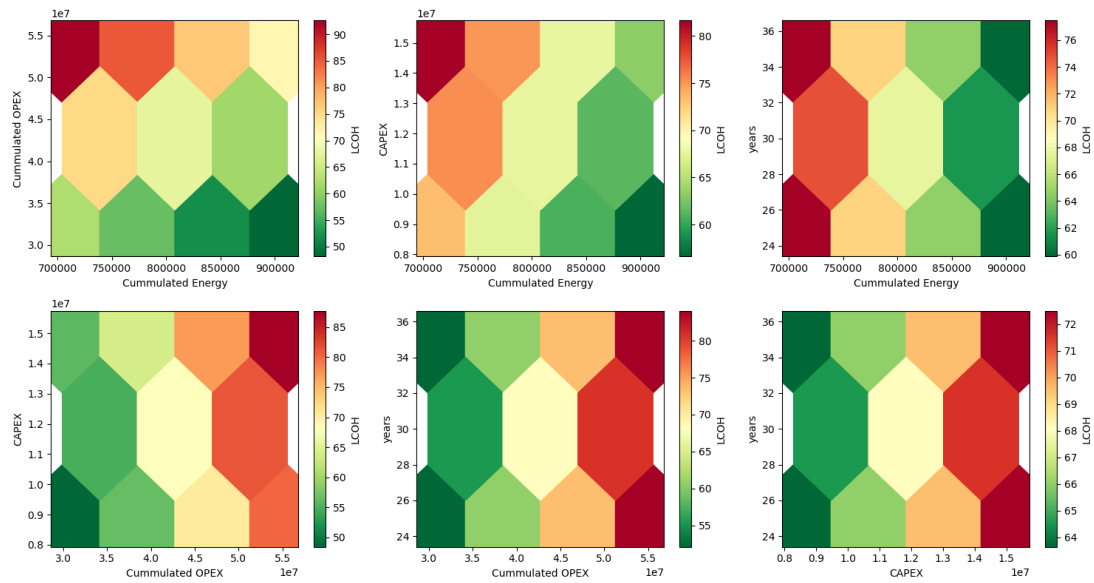


Figure 12 LCOH-Sensitivity Analysis created with the sensitivity package. LCOH is depicted in €/MWh, Energy in MWh, Capex & Opex in €

The sensitivity analysis in Figure 12 has been done with an open source package called sensitivity (Nick DeRobertis, 2022). This package presents the opportunity to simulate one formula or a function with multiple parameters at once. The simulated scenarios show that the operational expenditures have the biggest impact on the LCOH, as it yields the largest range within the highest and lowest LCOH with 90 and 65 €/MWh. The initial values for CAPEX, OPEX and the cumulated energy are from the base case scenario after a 30-year period.

The results of this sensitivity analysis bring a valuable insight into the system's resilience to economic fluctuations and highlight areas where strategic adjustments can be made. This forward-looking approach ensures that our system is not only efficient in its current operational context but also adaptable to the dynamic economic landscape.

### 3.4 Sensitivity of the modflow inputs

Since the grid-layout of the model is set to be constant, it was important to test the boundaries created by the thermal radius of the wells. The calculated thermal radius for the initial setup of 637.000 m<sup>3</sup> and a thickness of 50m has resulted in a thermal radius of approximately 132,2m. With the rule of multiplying, it by the factor 3,5, the distance between the wells has been set to 500m.

The next step was to track the outcome of an increased production rate (4000m<sup>3</sup>/day), and a lowered cut-off temperature(40°C), these parameters would increase the thermal radius to 142m



barely fitting into the grids layout. The various cases will be addressed as numbers within a bracket e.g. (1), (2).

Table 4 Sensitivity inputs for the modflow model scenarios.

Case Nr.	Production rate (m <sup>3</sup> /day)	Reservoir Thickness (m)	Cut-Off Temperature (°C)
1 (initial setup)	3500	50	50
2	3500	75	50
3	3500	50	40
4	3500	75	40
5	4000	50	50
6	4000	75	50
7	4000	50	40
8	4000	75	40

The results, indicating no breakthrough during the production period, can be directly reviewed in ModelMuse Figure 13 or through the extracted values from OBS-package or through the extracted values from the OBS-package.

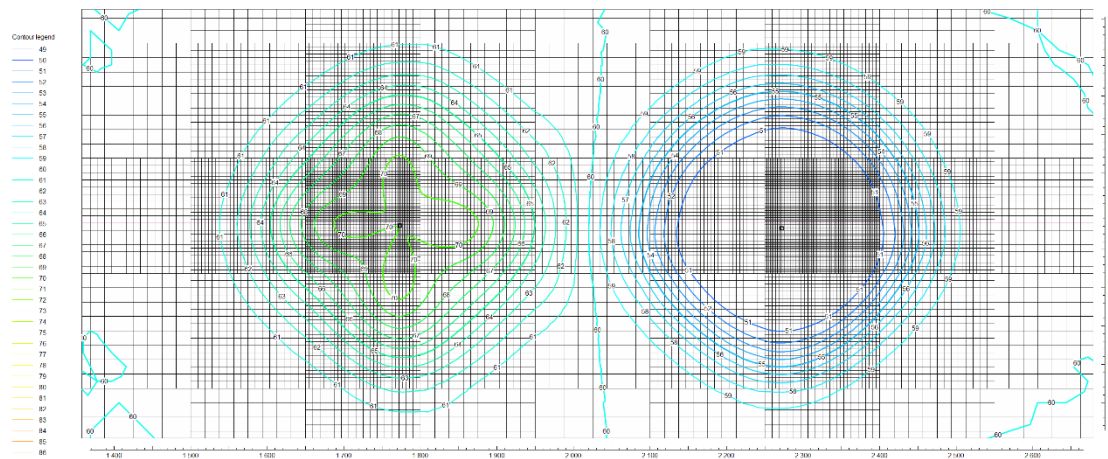


Figure 13 ModelMuse graphical interpretation of the concentrations/temperature from the top view, providing an insight for the result after 730 days.

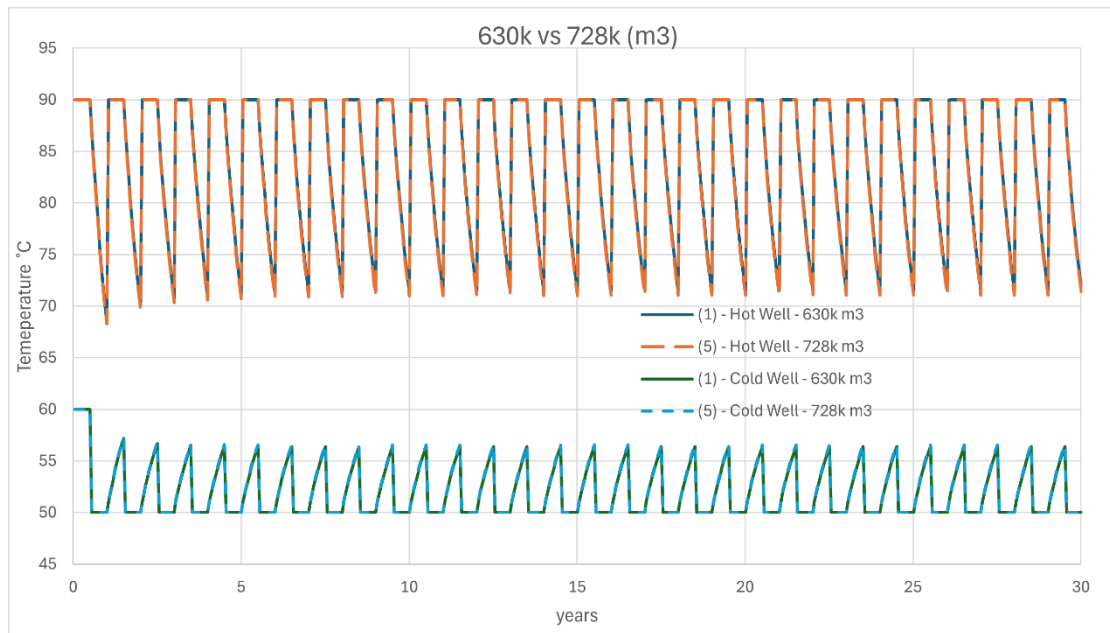


Figure 14 Temperature profile comparison between the different volumetric scenarios (case 1&5) of both hot and cold wells. 630k and 728k represent the value of total production in one production period (one year). Additional figure with a higher resolution for the Hot Wells can be found in the Appendix A Figure 27.

Plotting the retrieved temperatures from the wells for both volumetric scenarios (case 1 & 4) reveals that the temperatures are extremely close to each other. While analyzing the results directly in the CSV files expose that there are slight differences, the small time-steps chosen for each period are making it imprecise for plotting. In contrast to this, the recovery efficiencies results are more distinguished.

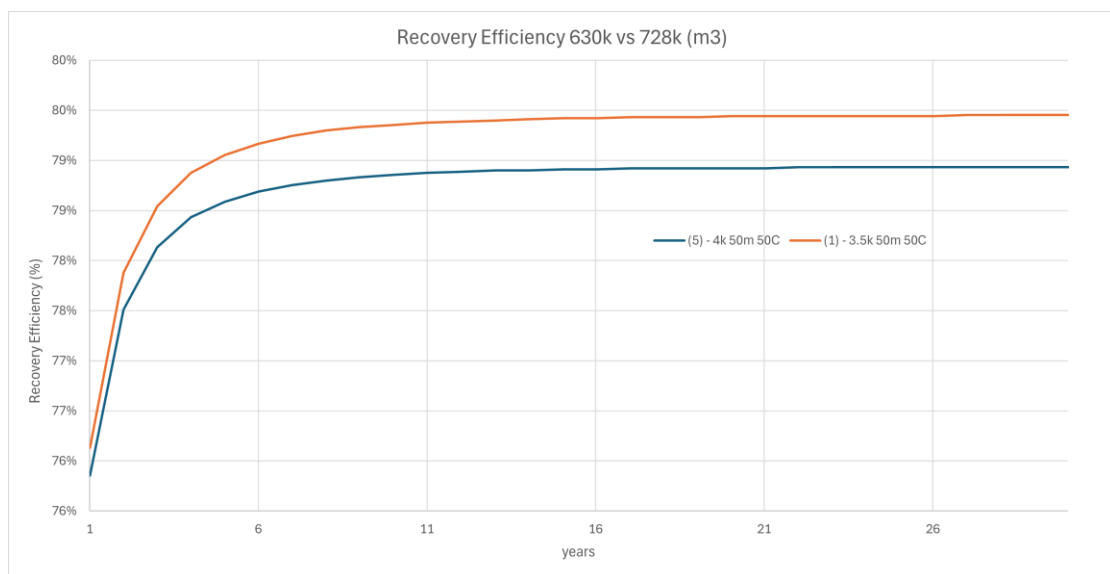


Figure 15 Recovery efficiency comparison of the different volumetric case scenario (case 1&4) results. 50m representing the reservoir thickness and 50°C the cut-off temperature.

Given the thermal radius is affected by the total screen length, the thickness of the reservoir has been increased to 75m (cases 2,4,6 and 8), although this is still insufficient for an optimal screen length of 91,75m and 87,4m, respectively (Equation 2.3). In a case of a real world scenario, the optimal screen length is often not reachable due to the present geology (Bloemendal and Hartog, 2018), which is why the screen length is not increased any further. The findings of this raise illustrate a significant growth in recovery efficiency for both production rate scenarios (case 2&6). Notably, the lower production rate (case 2) still returns the highest efficiency. This suggests that the cold well still has an impact on the temperatures extracted by the hot well producing 4000k m<sup>3</sup>/day.

Further simulations have been done with the cut-off temperature of 40°C (cases 3,4,7 and 8). As was expected, this change has not had a large influence on the outcoming recovery efficiencies, and the results are close to their initially produced temperatures.

In total, eight varying scenarios have been simulated with ModelMuse (Table 4). The expectations were that the outcomes would lean toward an increased production rate, even though the reservoir configuration was not initially designed for this capacity. But the Figure 17 proves, that the primary production rate still comes ahead. This underscores the pivotal role played by the reservoir and model configuration, hence the superior recovery efficiency of the smaller volume without an increased temperature cutoff (case 2) over an increased production rate.

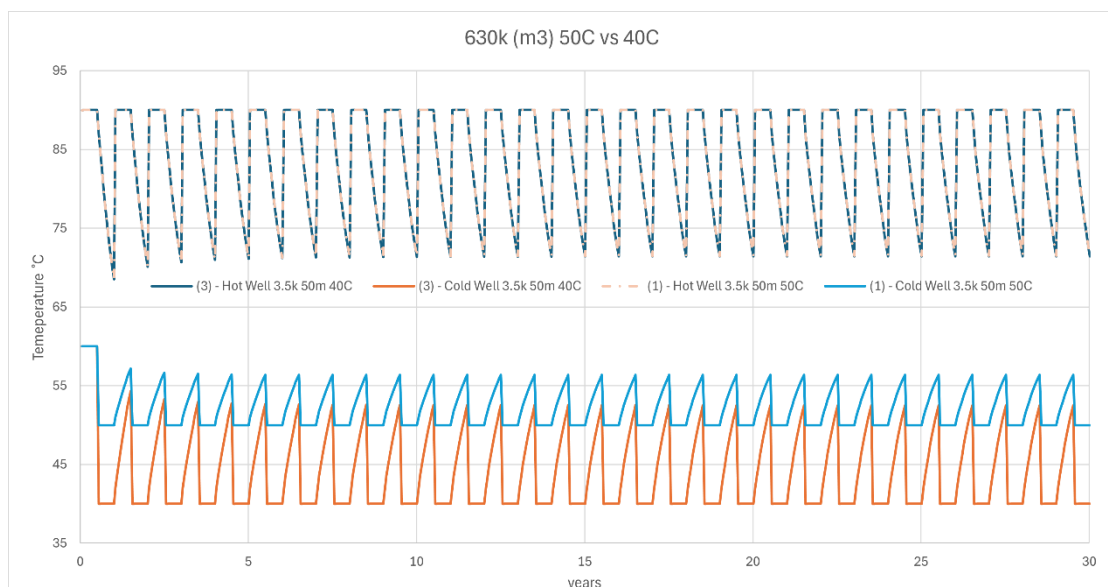


Figure 16 Temperature comparison with constant reservoir thickness of 50m and production rate 3500m<sup>3</sup>/day. The cut-off temperatures set to 50°C and 40°C.

Although the reservoir thickness is positively affecting the recovery efficiency and for all cases increasing it by 5%. The cut-off temperature, on the other hand, has a negative impact and decreases it by 0,1%.

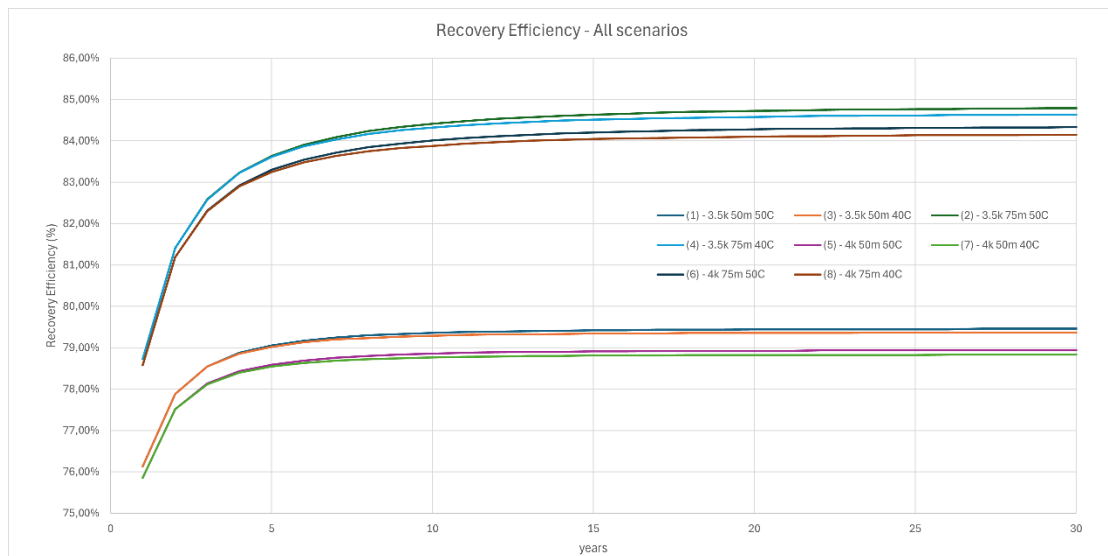


Figure 17 Recovery efficiency of all the simulated scenarios. The legend represents the production rate of 3.5k-4k m<sup>3</sup>/day, 40-50°C cut-off temperature and the reservoir thickness of 50-75m.

### 3.5 LCOH Results

The declining levelized costs of heat correspond to the rise in the reservoir thickness, a trend consistent with the findings from the Geneva case study (Daniilidis et al., 2022) This relationship is directly linked to transmissivity, which is the product of permeability and thickness. Even though the presented study maintains a constant permeability across all the simulated cases, the results underscore that the reservoir thickness stands out as one of the most critical factors in sizing up the LCOH outcomes.

Nevertheless, it is important to note that these positive outcomes do not mirror the increasing recovery efficiency. This is because the reduced cut-off temperature plays a substantial role in influencing the cumulated energy provided by the system.

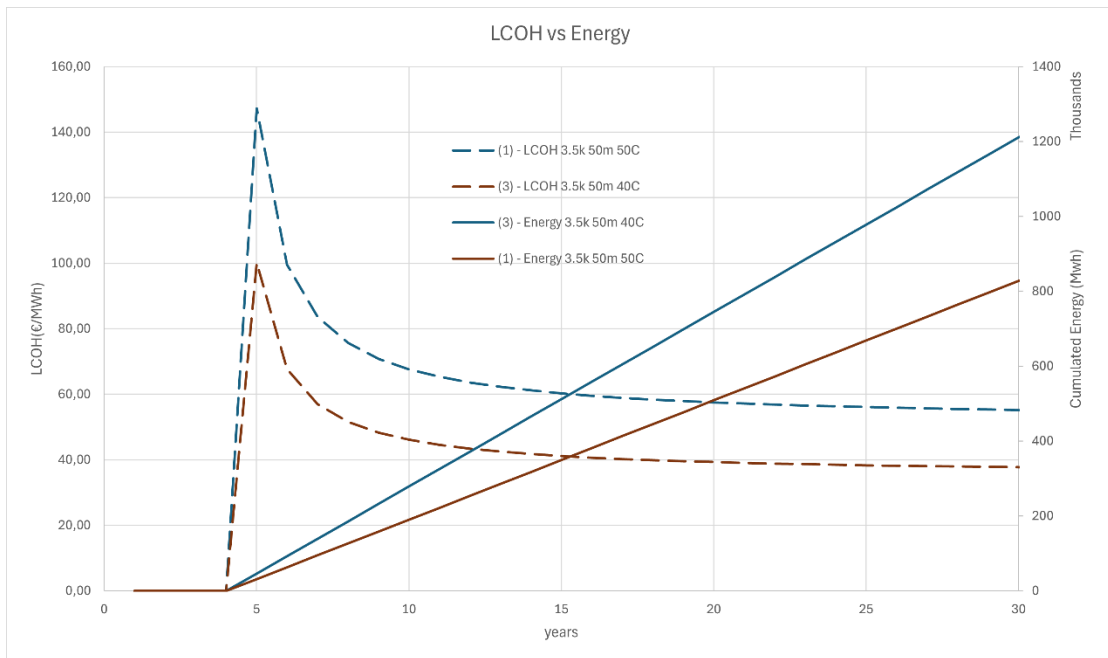


Figure 18 Shows the impact due to the variation in cut-off temperature, on the overall cumulative energy provided by the system and the effect on the LCOH outcome.

Clearly, LCOH is not only affected by the surface and reservoir conditions but also by the economic facet of the project, as has been simulated via a sensitivity analysis in the prior chapter.

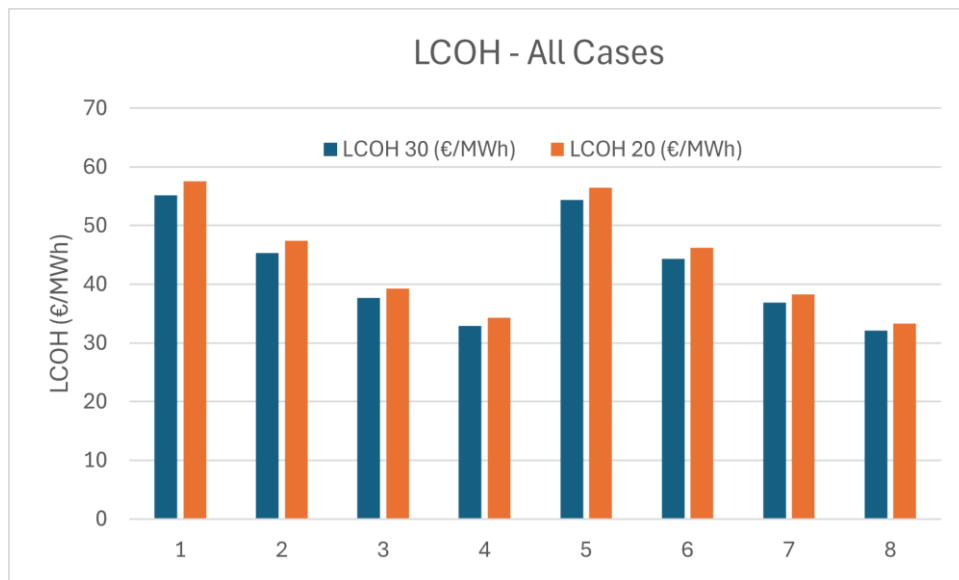


Figure 19 LCOH comparison for all the cases shown in Table 5 and the impact of 10-year change.

For the depicted base case (case 1) in the Figure 18, the LCOH results are 55,17€/MWh after 30 years and for the lowered cut-off temperature (case 3) the LCOH is sitting at 37,71€/MWh which is almost a 31,6% decrease. In energy terms, the scenario (1) yields around 829 GWh of

cumulated energy after 30 years and the scenario (3) 1212 GWh, clarifying the reduction in LCOH.

*Table 5 LCOH – All scenarios in comparison, being referred to as cases 1 to 8.*

Q (m3/day)	Cut-Off Temperature (C°)	Thickness(m)	LCOH(€/MWh)	LCOH(€/MWh)
			30 years	20 years
3500	50	50	55,17	57,51
3500	50	75	45,33	47,39
3500	40	50	37,71	39,28
3500	40	75	32,87	34,31
4000	50	50	54,34	56,43
4000	50	75	44,36	46,18
4000	40	50	36,91	38,31
4000	40	75	32,06	33,33

### 3.6 Net Present Value

The cumulated cashflow of the project is crucial for the calculation of the Net Present Value, as it represents the inflows and outflows of cash over time. The accuracy of this calculation is reflected on the precise cash flow projections making it essential to account for various sensitivity variables. A sensitivity analysis was conducted to identify the parameters that have the most significant impact on cash flow. It was only necessary to perform one analysis for a particular scenario as the projection's outcome can be assumed the same for all other cases.

Based on the cumulative cash flows, the NPV was calculated for each scenario as represented in the Figure 20.

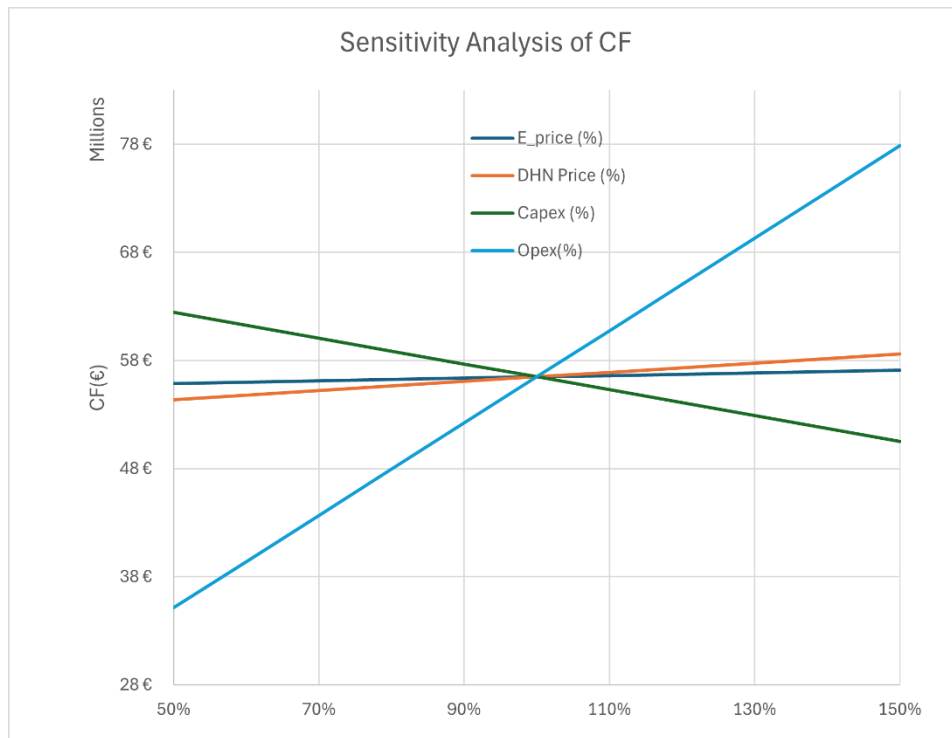


Figure 20 Cash-flow sensitivity analysis for the variables: CAPEX, OPEX, DHN-Price and the electricity Price.

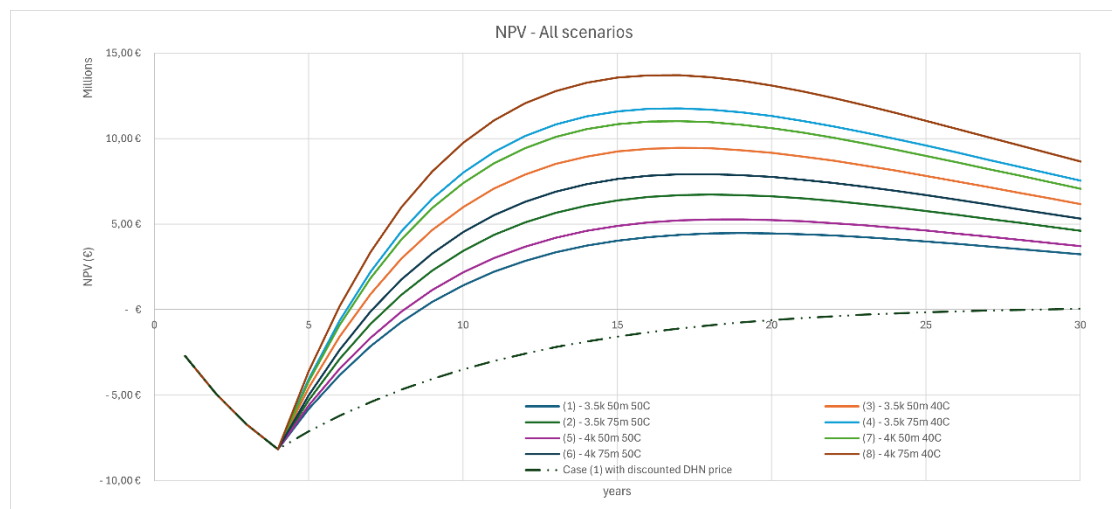


Figure 21 NPV-Comparison between all the simulated cases. The legend represents the production rate of 3.5k-4k m3/day, 40-50°C cut-off temperature and the reservoir thickness of 50-75m. Additionally the base case scenario (case 1) with discounted DHN price has been added to the plot for analogy.

Similarly to the LCOH results, the NPV may not align with the system's efficiency, given that the scenario with the highest NPV differs from the one with the highest efficiency. This behaviour arises because the augmented production rate is directly linked to an increase in energy output. Despite greater temperature disparities in alternative scenarios, the production rate remains the dominant factor. The adjustments in production rate and temperature play a key role in the shaping of the timeline for achieving a positive cash flow within the project. A

higher production rate accelerates the influx of revenue, shortening the expectation time for a positive cash flow. Additionally, the variations in the temperature cut-offs impact the operational efficiency and simultaneously increase the potential energy output of the system.

The actual selling price of energy emerges as a key factor for a favorable NPV outcome. In the base case scenario, as mentioned earlier, it is assumed to be no-cost energy, although this is highly improbable in real-life situations. Furthermore, a calculation has been conducted to illustrate the influence of research and development time on the discounted DHN price.

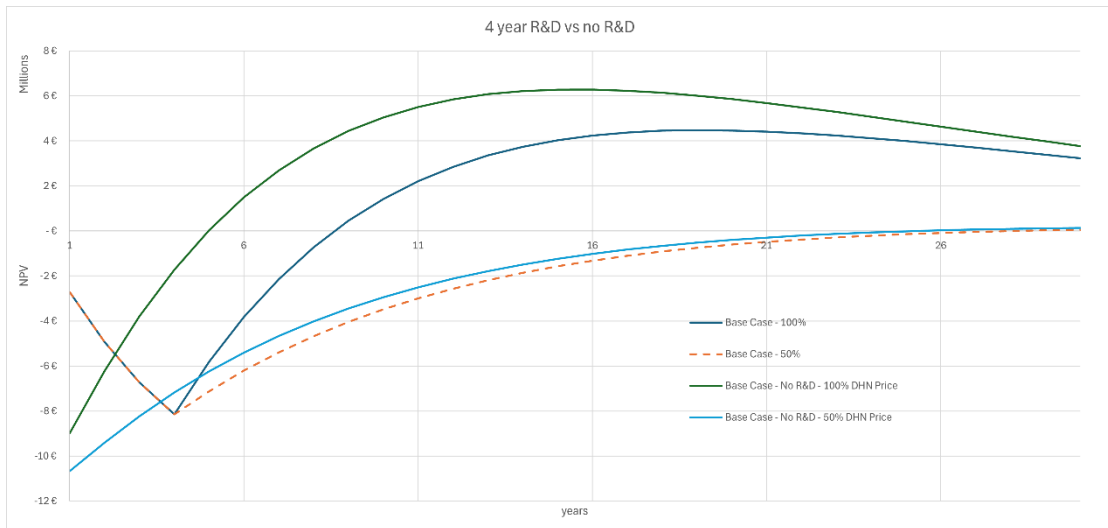


Figure 22 The impact of discounting the DHN-price and no research and development time.



## Chapter 4

### Discussion

The success of this simulation is provided by the resulting temperature profile of the configured ATES System. The varying modflow input parameters reveal a substantial influence over the recovery efficiency, LCOH and NPV. The results highlight the significant importance of the thermal radius in designing an ATES, as it plays a key role in maintaining high recovery efficiency. Achieving an ideal screen length is presented as a challenge, as many of the targeted aquifers do not yield that desired thickness. This can be an issue if there is a desire to increase the production rate. Additionally, the discrepancies between the results in efficiency and the economics parameters indicate the need for additional scenarios to comprehensively analyze the system dynamics.

The resulting temperature profile offers an overview of the system's efficiency and power output. The LCOH estimation emphasizes the importance of planning HT-ATES for an extended period, showcasing significant improvements over time. The results can be compared with the TU-Delft Campus case study (T.M.G. van de Griendt, 2022) where the projected LCOH after 30 years reached 52 €/MWh. While comparing with other various space and water heating technologies from an IEA study for Germany (IEA, 2024) (as to writers knowledge there is no present data for Austria), HT-ATES outperforms all of them. This further validates the competitiveness of HT-ATES among heating technologies. The sensitivity analysis confirms that opex is the most influential variable, which could be expected being it almost four times larger than a capex. While estimating appropriate capex is crucial, it is highly site-specific, considering numerous influencing factors, such as legal fees, insurance costs, property taxes, and more.

On the other hand, recovery efficiency, LCOH, and Net Present Value (NPV) exhibit variable behavior when testing various dimensions of the Modflow base model. Recovery efficiency is predominantly affected by the layout, with reservoir thickness having the most substantial impact. In contrast, LCOH and NPV are significantly influenced by enhanced production rates. Due to the necessary assumptions made regarding the geological parameters, the impact on simulation results might differ by a large margin while creating other scenarios.

To the best of the writer's knowledge, there are no cases simulating heat transportation with ModelMuse. Despite this, the simulation results demonstrate a viable outcome. This paper can potentially open the way for subsequent testing.

## Chapter 5

### Conclusion

Although the results of this assessment suggest a positive outlook for the proposed approach, it is crucial to acknowledge existing limitations. The proposed model allows for a quick assessment of the temperature behavior in a given reservoir, but further incorporation of missing aspects and parameters is necessary to transform it into a definitive decision-making tool. Modflow proves to be a powerful and versatile tool, capable of simulating specific scenarios with proper reservoir configuration and provided data. The current settings enabled the simulation of a simplified heat transportation case-study, as proposed in previous versions of Modflow and the additional SEAWAT. To achieve more precise results, obtaining actual geological parameters from the area and implementing further dependencies is essential.

Recognizing the importance of openness and accessibility, this HT-ATES simulation relies solely on an open-source model. This not only facilitates universal usage but also encourages collaborative improvements in aquifer-system simulations. There is a large potential for the ModelMuse GUI to become a versatile, free-to-use tool for aquifer-system simulations if it incorporates new packages. However, if not, there is a necessity to extend the model by implementing packages supported only by the Python environment FloPy. Despite FloPy's excellence in Modflow modeling, it lacks support for the CTS package, which was the crucial package for the simulation of dynamic concentration flow in this ATES scenario. There are also other variants offering the modflow model, only in most cases these are not free to use. It would be highly beneficial if the packages from ModelMuse would align with the python environment of FloPy, as it would elevate the evaluation of results.

In future studies, it would be of interest to create a similar simulation with the same parameters in FloPy. In this case, instead of using the CTS package, which was used in ModelMuse, manual reading of concentration file would be necessary to further pass these results each step to the WEL, GHB and SSM package.

If the simulation yielded similar results to the ModelMuse case, it would be engaging to create a dynamic iteration with additional parameters. This would result in more advanced sensitivity analysis, as other subsurface parameters could be added.

During the simulations only one subsurface parameter was varying which was the thickness of the reservoir, but other variables, which have an impact on the groundwater flow should be considered. As an example, all these can be simulated in the FloPy environment:

- Groundwater flow/movement.
- Sorption or losses to other layers.
- Density driven flow based on density-temperature correlation.
- Viscosity-Temperature correlation.

Economic feasibility should not be the only decision-making parameter. Due to the increased interest in the decreasing GHG, it would be of interest for future studies to add a comparison-variable where the amount of CO<sup>2</sup> emissions savings is compared to other conventional heating methods.

---

## References

- Bedekar, V., Morway, E. D., Langevin, C. D. and Tonkin, M. J. (2016) *Techniques and Methods*.
- Bloemendal, M. and Hartog, N. (2018) ‘Analysis of the impact of storage conditions on the thermal recovery efficiency of low-temperature ATES systems’, *Geothermics*, vol. 71, pp. 306–319.
- Bloemendal, M., Jaxa-Rozen, M. and Olsthoorn, T. (2018) ‘Methods for planning of ATES systems’, *Applied Energy*, vol. 216, pp. 534–557.
- C. D. Langevin, D. T. Thorne Jr, A. M. Dausman, M. C. Sukop and Weixing Guo (2008) *SEAWAT Version 4: A Computer Program for Simulation of Multi-Species Solute and Heat Transport*.
- Daniilidis, A., Mindel, J. E., Oliveira Filho, F. de and Guglielmetti, L. (2022) ‘Techno-economic assessment and operational CO<sub>2</sub> emissions of High-Temperature Aquifer Thermal Energy Storage (HT-ATES) using demand-driven and subsurface-constrained dimensioning’, *Energy*, vol. 249, p. 123682.
- Dirk Schulze-Makuch (2005) ‘Longitudinal dispersivity data and implications for scaling behavior’, *Ground Water*, vol. 43, no. 3, pp. 443–457 [Online]. Available at <https://go.gale.com/ps/i.do?p=AONE&u=googlescholar&id=GALE|A133188538&v=2.1&it=r&sid=AONE&asid=50b35088>.
- E-Control (2024) *Was kostet eine Kilowattstunde Strom? - E-Control* [Online]. Available at <https://www.e-control.at/konsumenten/strom/strompreis/was-kostet-eine-kwh> (Accessed 19 January 2024).
- Geologische Bundesanstalt (2015) *Erläuterungen zur geologischen Themenkarte Thermalwässer in Österreichs, Wien*.
- FFG Projektdatenbank (2023) *ATES Vienna* [Online]. Available at <https://projekte.ffg.at/projekt/3849155> (Accessed 26 November 2023).
- Fleuchaus, P., Godschalk, B., Stober, I. and Blum, P. (2018) ‘Worldwide application of aquifer thermal energy storage – A review’, *Renewable and Sustainable Energy Reviews*, vol. 94, pp. 861–876.

---

Fleuchaus, P., Schüppler, S., Stemmler, R., Menberg, K. and Blum, P. (2021) 'Aquiferspeicher in Deutschland', *Grundwasser*, vol. 26, no. 2, pp. 123–134.

GBA MapViewer (2017) [Online]. Available at [https://gisgba.geologie.ac.at/gbaviewer/?url=https://gisgba.geologie.ac.at/arcgis/rest/services/AT\\_GBA\\_PROFILE/MapServer](https://gisgba.geologie.ac.at/gbaviewer/?url=https://gisgba.geologie.ac.at/arcgis/rest/services/AT_GBA_PROFILE/MapServer) (Accessed 31 January 2024).

Gier, S., Worden, R. H., Johns, W. D. and Kurzweil, H. (2008) 'Diagenesis and reservoir quality of Miocene sandstones in the Vienna Basin, Austria', *Marine and Petroleum Geology*, vol. 25, no. 8, pp. 681–695.

GitHub (2024) GitHub - modflowpy/flopy: A Python package to create, run, and post-process MODFLOW-based models [Online]. Available at <https://github.com/modflowpy/flopy> (Accessed 4 January 2024).

Godschalk, B. and Oerlemans, P. (2021) First results of the full scale HT-ATES project in a greenhouse area Middenmeer in the Netherlands.

Harzhauser, M., Kranner, M., Mandic, O., Strauss, P., Siedl, W. and Piller, W. E. (2020) 'Miocene lithostratigraphy of the northern and central Vienna Basin (Austria)', *Austrian Journal of Earth Sciences*, vol. 113, no. 2, pp. 169–199.

Heatstore (2021) HT-Ates Project - Bern [Online]. Available at <https://www.heatstore.eu/national-project-switzerland-bern.html> (Accessed 26 November 2023).

HydroSOLVE, Inc. (2019) Hydraulic Properties :: Aquifer Testing 101 [Online]. Available at [http://www.aqtcsolv.com/aquifer-tests/aquifer\\_properties.htm](http://www.aqtcsolv.com/aquifer-tests/aquifer_properties.htm) (Accessed 14 January 2024).

Chen, J. M. (2021) 'Carbon neutrality: Toward a sustainable future', *Innovation (Cambridge (Mass.))*, vol. 2, no. 3, p. 100127.

IEA (2024) Levelized cost of heating (LCOH) for consumers, for selected space and water heating technologies and countries –&nbsp;Charts – Data & Statistics - IEA [Online], IEA. Available at <https://www.iea.org/data-and-statistics/charts/levelized-cost-of-heating-lcoh-for-consumers-for-selected-space-and-water-heating-technologies-and-countries> (Accessed 24 January 2024).

IEA SHC || Task 54 || LCoH Tool (2024) [Online]. Available at <https://task54.iea-shc.org/lcoh-tool> (Accessed 4 January 2024).

Karlsruhe Institute of Technology (2023) KIT - DeepStor [Online]. Available at <https://www.geoenergicampus.kit.edu/deepstor.php> (Accessed 26 November 2023).

- Langevin, C. D., Hughes, J. D., Banta, E., Provost, A., Niswonger, R. and Panday, S. (2017) MODFLOW 6, the U.S. Geological Survey Modular Hydrologic Model [Computer program].
- Loibl, W., Stollnberger, R. and Österreicher, D. (2017) ‘Residential Heat Supply by Waste-Heat Re-Use: Sources, Supply Potential and Demand Coverage—A Case Study’, *Sustainability*, vol. 9, no. 2, p. 250.
- Lukawski, M. Z., Anderson, B. J., Augustine, C., Capuano, L. E., Beckers, K. F., Livesay, B. and Tester, J. W. (2014) ‘Cost analysis of oil, gas, and geothermal well drilling’, *Journal of Petroleum Science and Engineering*, vol. 118, pp. 1–14.
- Magistratsabteilung 20, E. (2022) ‘Energiebericht der Stadt Wien: Berichtsjahr 2022’ [Online]. Available at <https://www.wien.gv.at/spezial/energiebericht/>.
- MATHIAS Harzhauser and Werner E. Piller (2005) ‘Neogen des Wiener Beckens’.
- Mindel, J. and Driesner, T. (2020) HEATSTORE: Preliminary Design of a High Temperature Aquifer Thermal Energy Storage (HT-ATES) System in Geneva Based on TH Simulations.
- MODFLOW 6 Documentation — MODFLOW 6 Program Documentation (2024) [Online]. Available at <https://modflow6.readthedocs.io/en/latest/index.html> (Accessed 31 January 2024).
- MODFLOW 6: USGS Modular Hydrologic Model | U.S. Geological Survey (2024) [Online]. Available at <https://www.usgs.gov/software/modflow-6-usgs-modular-hydrologic-model> (Accessed 7 January 2024).
- MT3D-USGS: Groundwater Solute Transport Simulator for MODFLOW | U.S. Geological Survey (2024) [Online]. Available at <https://www.usgs.gov/software/mt3d-usgs-groundwater-solute-transport-simulator-modflow> (Accessed 8 January 2024).
- Nick DeRobertis (2022) sensitivity 0.2.8 documentation [Online]. Available at <https://nickderobertis.github.io/sensitivity/api/modules.html> (Accessed 1 February 2024).
- SEAWAT: A Computer Program for Simulation of Three-Dimensional Variable-Density Ground-Water Flow and Transport | U.S. Geological Survey (2024) [Online]. Available at <https://www.usgs.gov/software/seawat-computer-program-simulation-three-dimensional-variable-density-ground-water-flow> (Accessed 8 January 2024).
- Schüppler, S., Fleuchaus, P. and Blum, P. (2019) ‘Techno-economic and environmental analysis of an Aquifer Thermal Energy Storage (ATES) in Germany’, *Geothermal Energy*, vol. 7, no. 1.
- ‘Stadt\_Wien\_Energiebericht\_2022’.
- T.M.G. van de Griendt (2022) Benefits of High-Temperature Storage for Base Load Geothermal Energy, MSc Thesis.

---

Takács, G. (2018) Electrical submersible pumps manual: Design, operations, and maintenance, Cambridge MA, Gulf Professional Publishing.

Tess Wegman (2017) HT-ATES System case study on TU Delft campus, Bachelor, Delft University of Technology.

ThermoGIS (2024) Economic model | Thermogis [Online]. Available at <https://www.thermogis.nl/en/economic-model> (Accessed 4 January 2024).

USGS (2023) MODFLOW and Related Programs | U.S. Geological Survey [Online]. Available at <https://www.usgs.gov/mission-areas/water-resources/science/modflow-and-related-programs> (Accessed 26 November 2023).

USGS (2024) ModelMuse: A Graphical User Interface for Groundwater Models | U.S. Geological Survey [Online]. Available at <https://www.usgs.gov/software/modelmuse-a-graphical-user-interface-groundwater-models> (Accessed 4 January 2024).

Wessely, G. and Draxler, I. (2006) Niederösterreich, Wien, Geologische Bundesanstalt.

Wien Energie (2023) Fernwärme beziehen für Business-Kunden | Wien Energie [Online]. Available at <https://www.wienenergie.at/business/produkte/waerme/fernwaerme/> (Accessed 29 August 2023).

Wien Energie (2024) Fernwärme anmelden » Umweltschonendes Heizen | Wien Energie [Online]. Available at <https://www.wienenergie.at/privat/produkte/waerme/fernwaerme/> (Accessed 19 January 2024).

Yoann Louvet, Stephan Fischer, Simon Furbo, Frederico Giovanetti, Michael Köhl, Franz Mauthner, Daniel Mugnier, Daniel Philippen and Francois Veynandt (2017) ‘A01-Info-Sheet-LCOH-for-Solar-Thermal-Applications: Guideline for levelized cost of heat (LCoH) calculations for solar thermal applications’.



# Appendix A

## A.1 Introduction Addition

Energy flow of the Vienna city from the year 2020 which depicts the dependency of DHN on the imported gas.

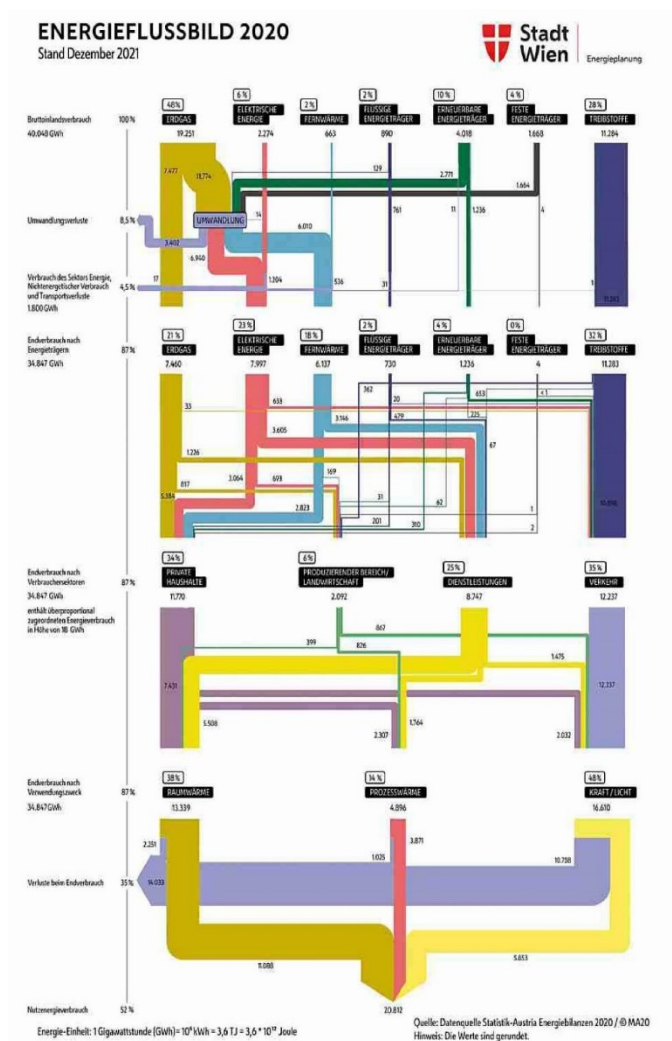


Figure 23: Energy Flow Vienna 2022 (Magistratsabteilung 20, 2022, p. 37)

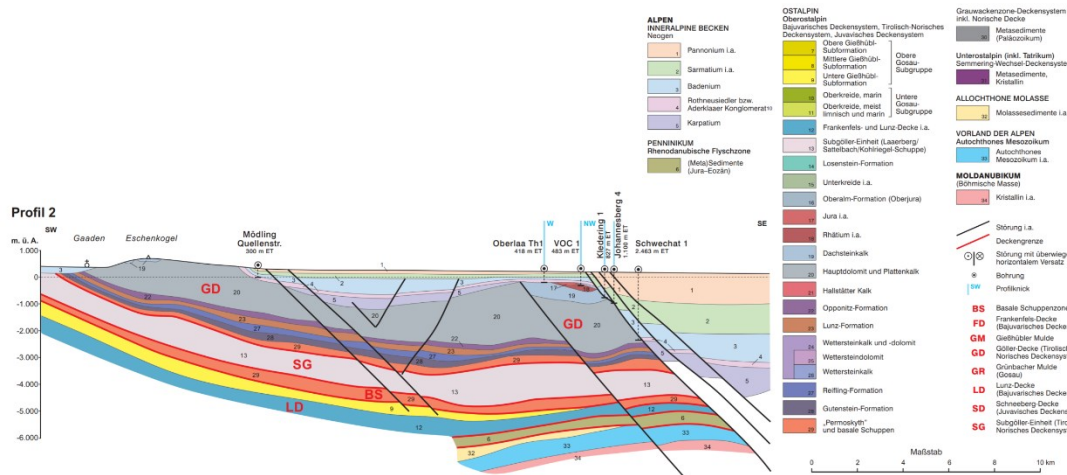


Figure 24 Cross section from the GBA website, depicting the Vienna Basin (GBA MapViewer, 2017; Geologische Bundesanstalt, 2015)

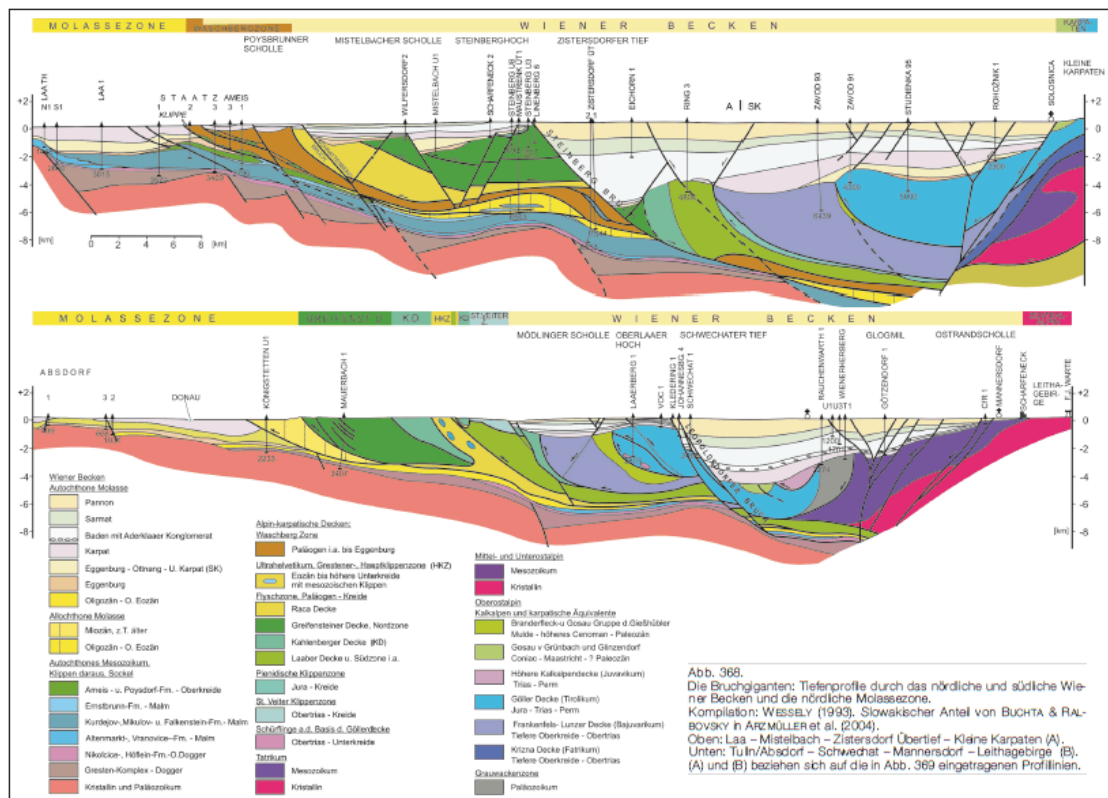


Figure 25 Cross section from the GBA website, depicting the Vienna Basin (GBA MapViewer, 2017; Geologische Bundesanstalt, 2015)

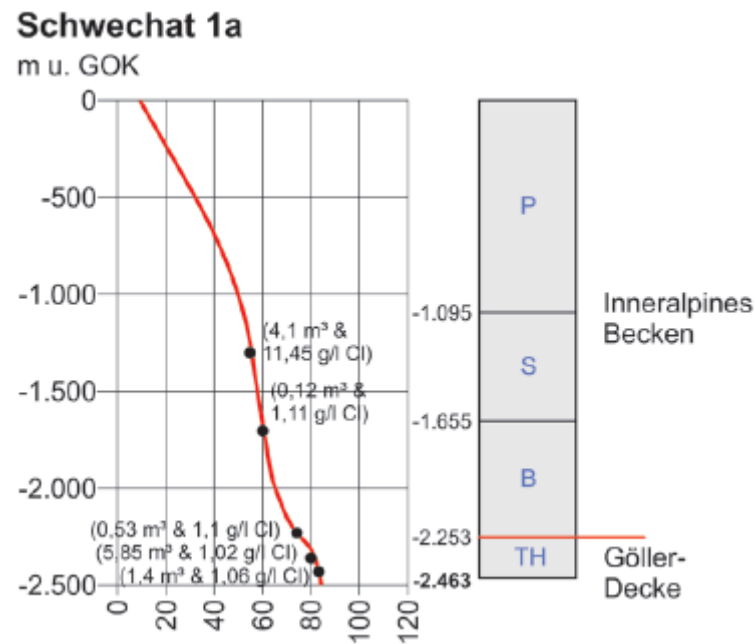


Figure 26 Well temperature profile from Schewacht 1a (Geologische Bundesanstalt, 2015; GBA MapViewer, 2017)

## A.2 FloPy

Although mf6 offers various packages, not all of them are yet implemented into the GUI of ModelMuse. Two packages especially would be of a larger interest for this particular case study, as the temperature affects other parameters regarding the temperature variation.

### A.2.1 BUY Package

The buoyancy package (BUY) allows the user to simulate variable density flow. This can be achieved by specifying the density, reference density and the slope defining the slope of the density-concentration, used in the equation of state. This results that the model will use variable-density form of Darcy's Law.

### A.2.2 VSC Package

To simulate the dependence of viscosity on the solute the viscosity package (VSC) has to be implemented. This results in the model accounting for the dependencies of viscosity on the changes in hydraulic conductivity and stress-package conductance.

Similarly, to the BUY package the user must define the reference viscosity, typically it can be fresh water at the temperature of 20 °C. For this specific case of temperature transport, the linear slope of how viscosity changes with temperature has to be specified.

Detailed explanation of how to structure the input files can be found in the mf6 input-output documentation (Langevin et al., 2017; MODFLOW 6 Documentation — MODFLOW 6 Program Documentation, 2024) .

### A.3 Results

The following Figure 27, depicts only the hot-well temperature profile for higher resolution, which reveals that the actual temperature of increased production rate reaches lower temperatures.

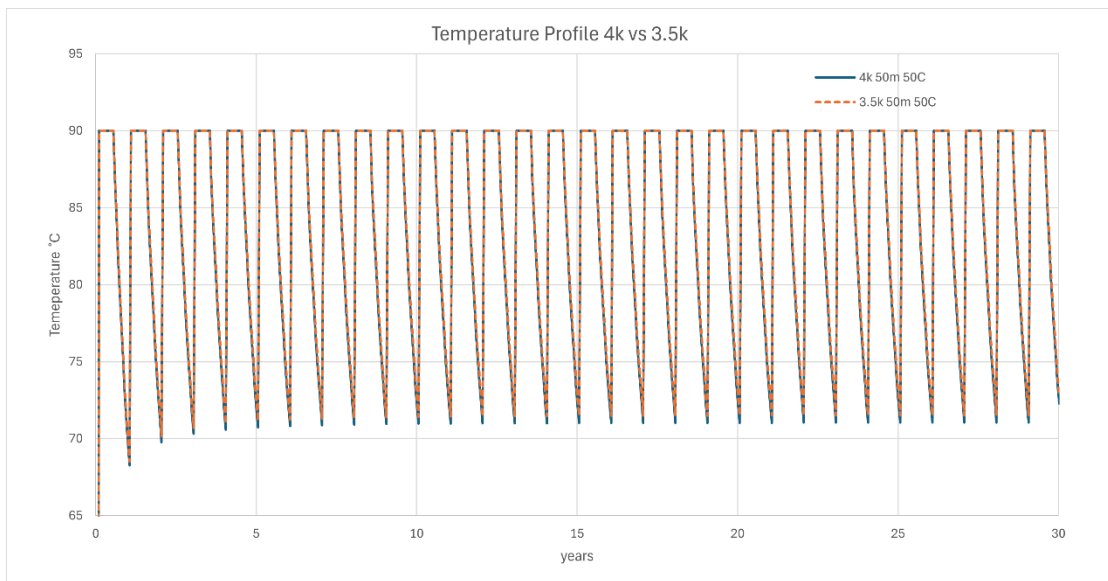


Figure 27 Temperature profile comparison between the hot wells of different volumetric scenarios.

#### A.3.1 ModelMuse Results

The following figure depicts the created grid with a higher resolution, which points at the importance of higher density of cells near the wells.

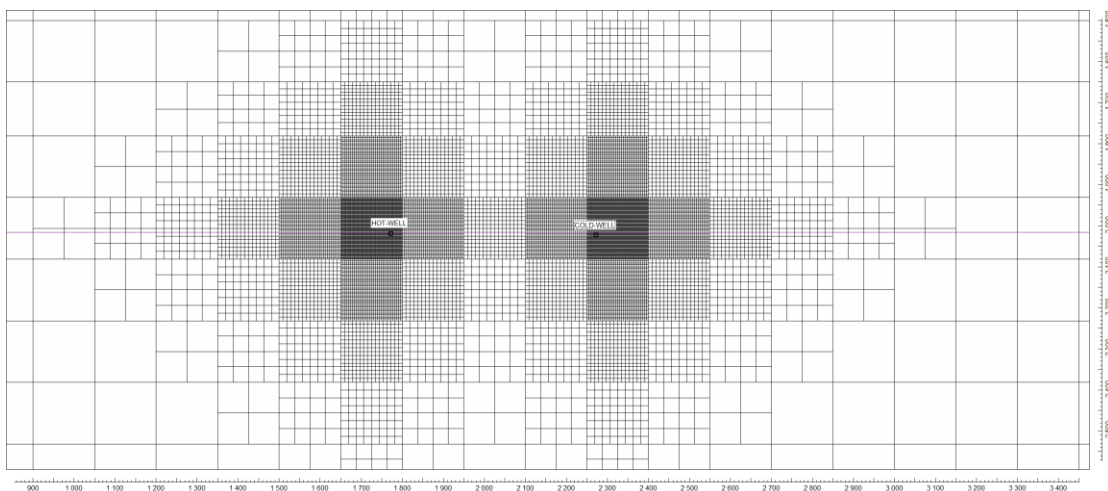


Figure 28 Close-up of the ModelMuse grid used for the simulation, depicting the Hot and the Cold wells.

ModelMuse exporting option allows the user to view each step of the simulation either as a contour data or color grid. This has been done to present the results of the first two periods.

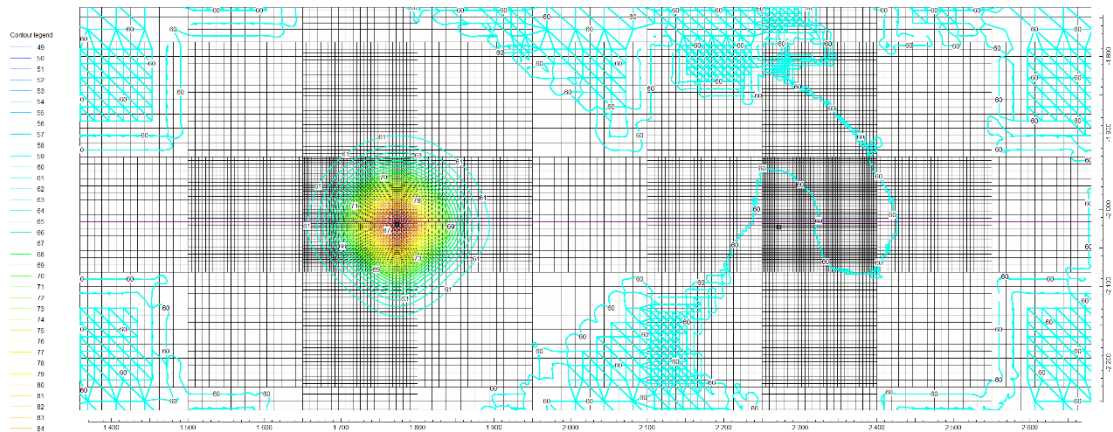


Figure 29 Period 1 Step 1

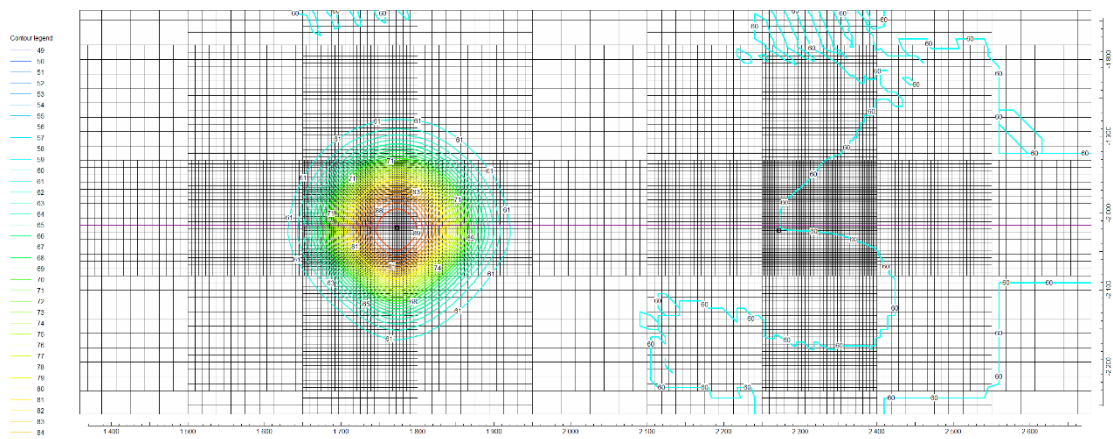


Figure 30 Period 1 Step 2

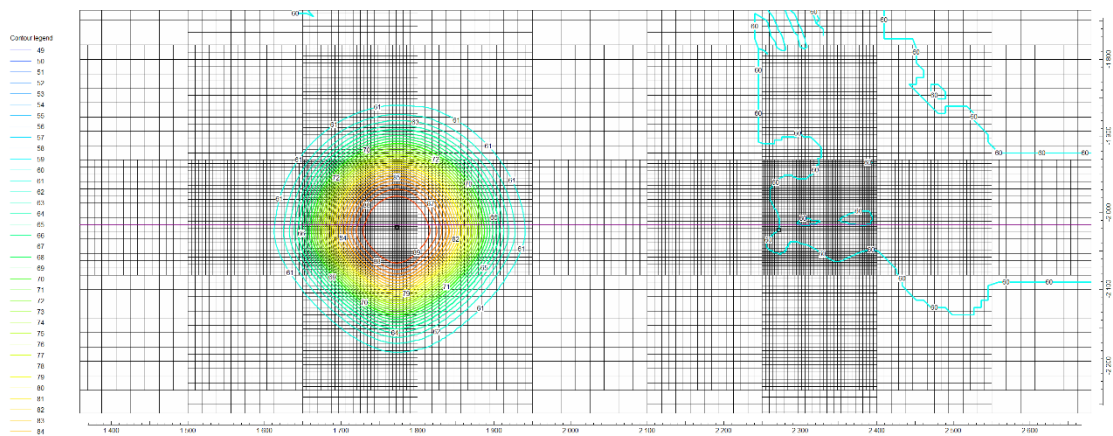


Figure 31 Period 1 Step 3



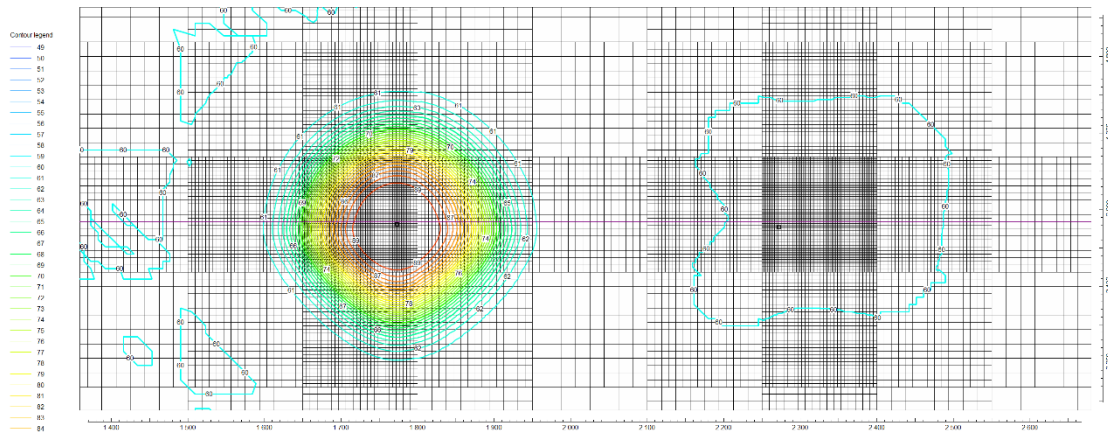


Figure 32 Period 1 Step 4

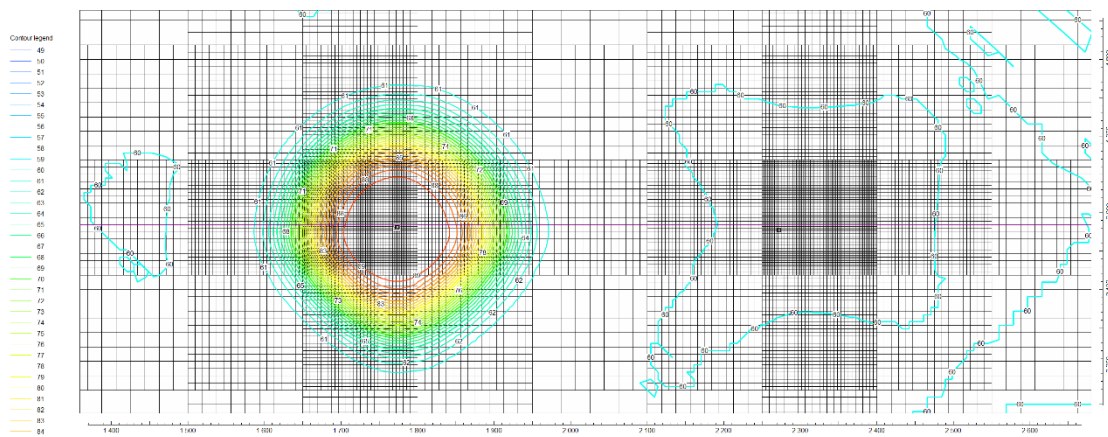


Figure 33 Period 1 Step 5

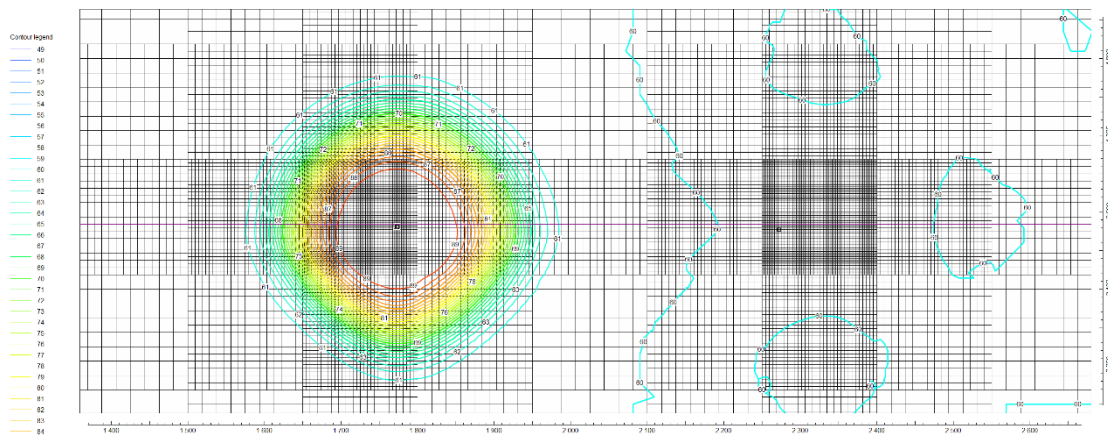


Figure 34 Period 1 Step 6

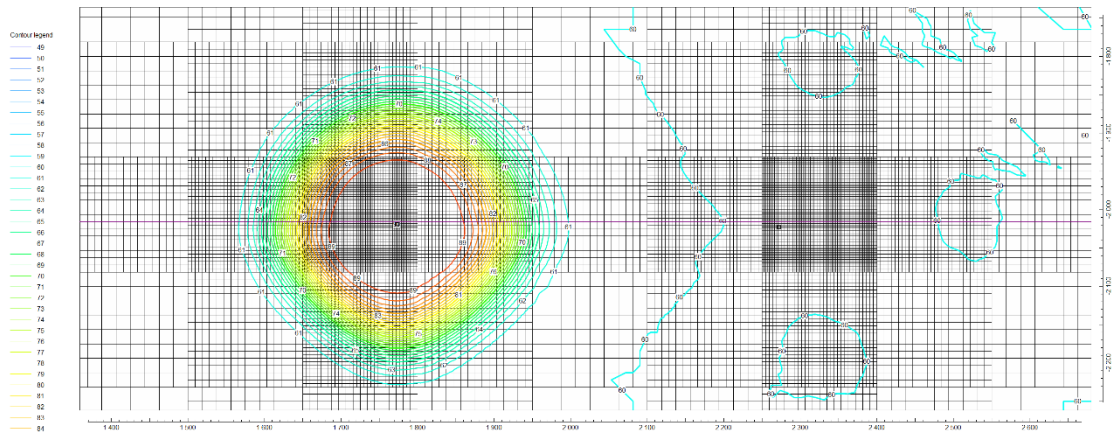


Figure 35 Period 1 Step 7

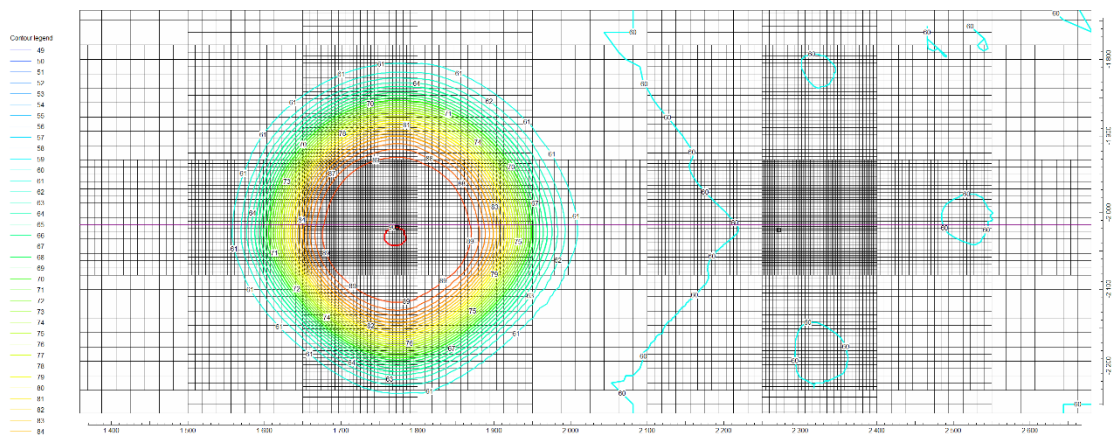


Figure 36 Period 1 Step 8

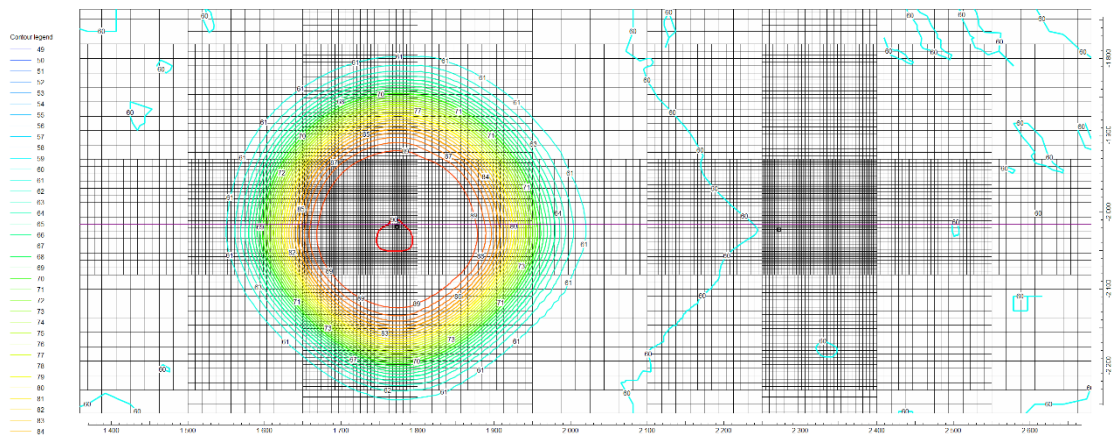


Figure 37 Period 1 Step 9

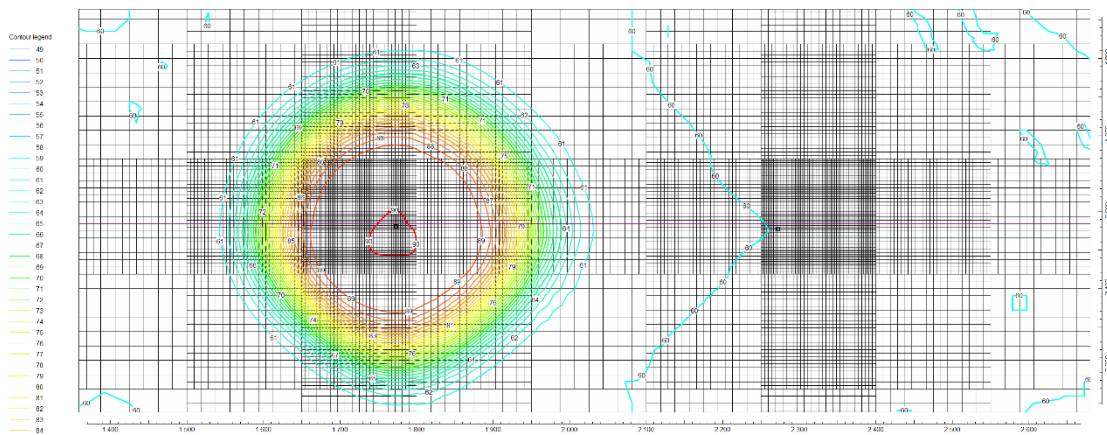


Figure 38 Period 1 Step 10

The 10<sup>th</sup> period ends the first injection period of HOT-water, resulting in a followed extraction period and injection in the COLD-Well.

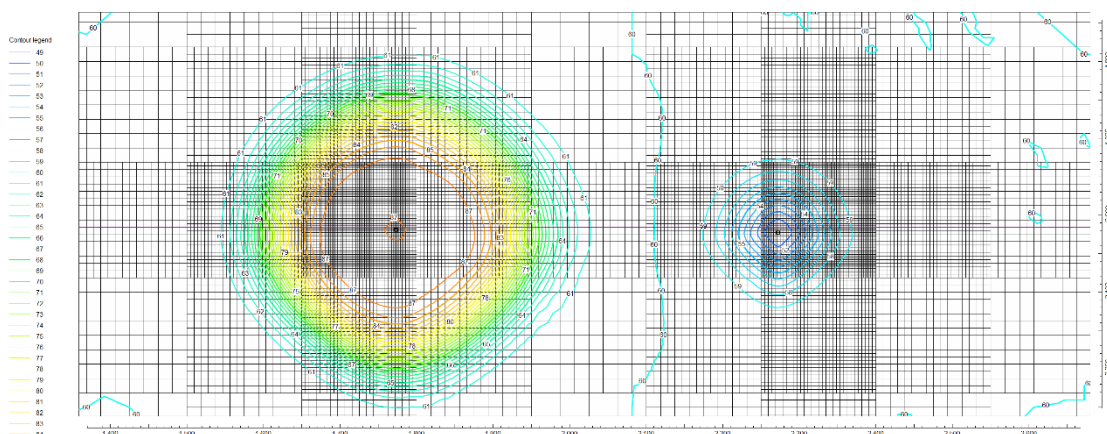


Figure 39 Period 2 Step 1

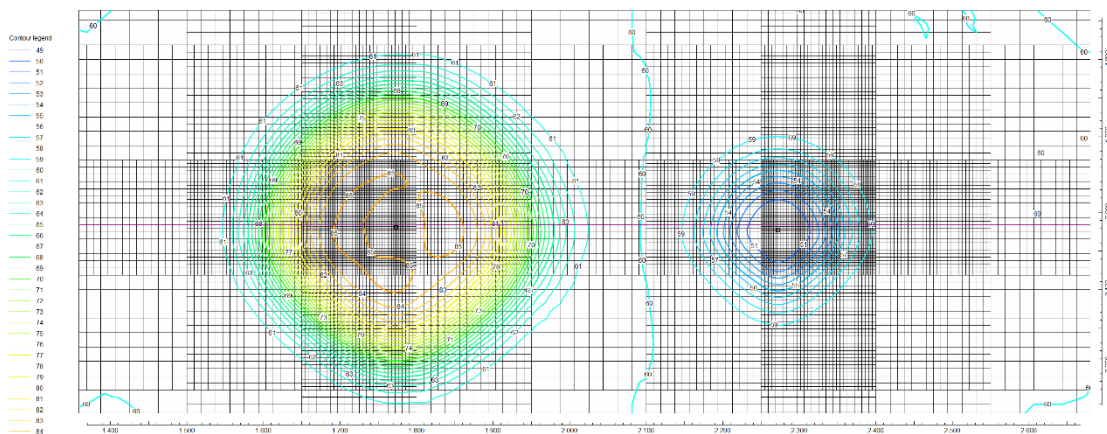


Figure 40 Period 2 Step 2



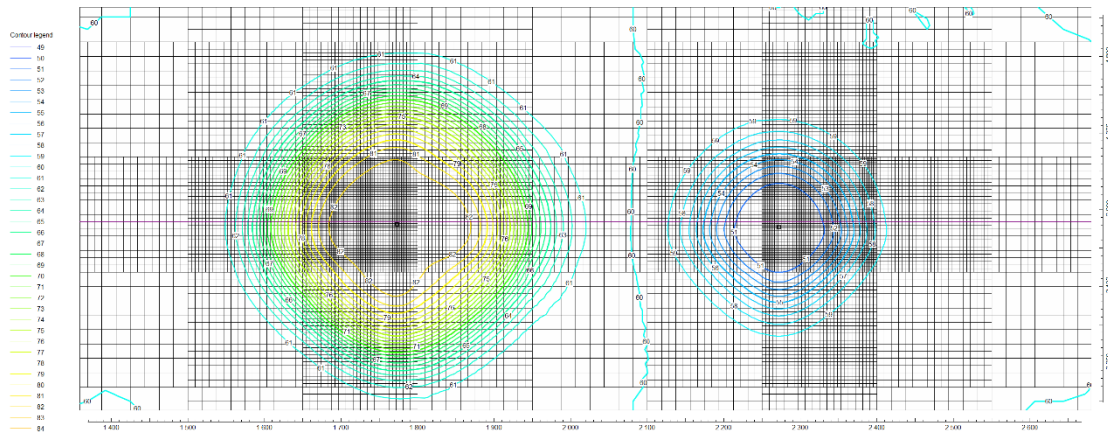


Figure 41 Period 2 Step 3

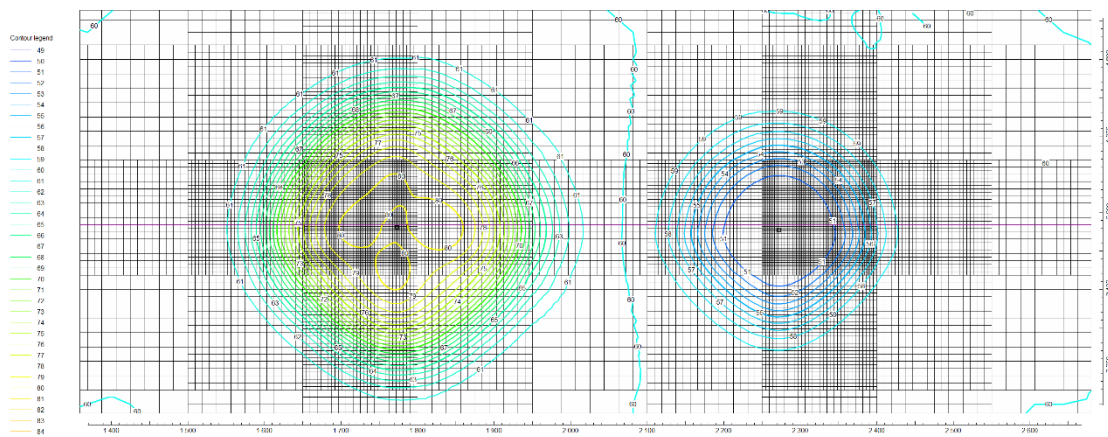


Figure 42 Period 2 Step 3

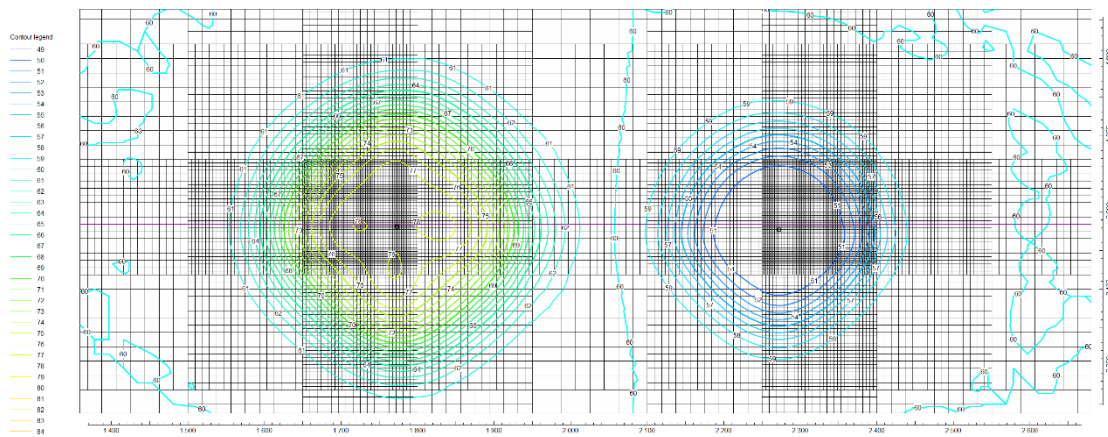


Figure 43 Period 2 Step 4

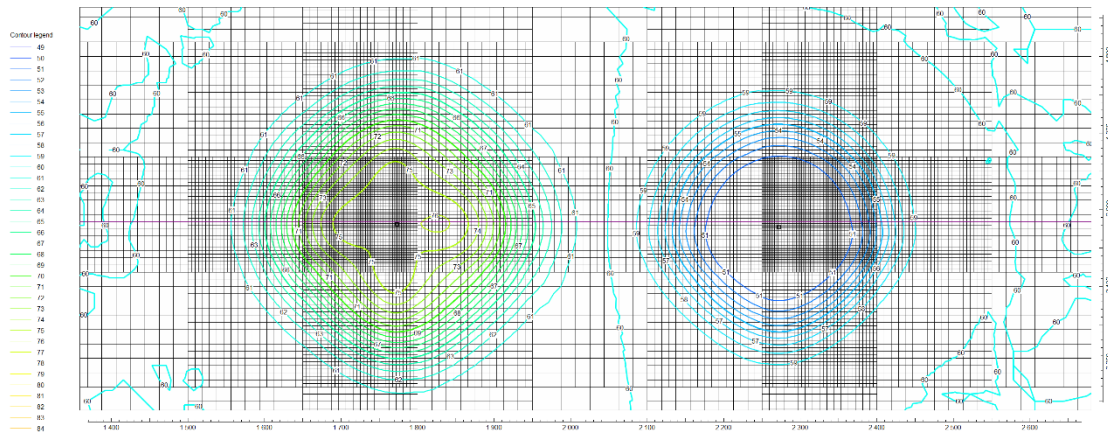


Figure 44 Period 2 Step 5

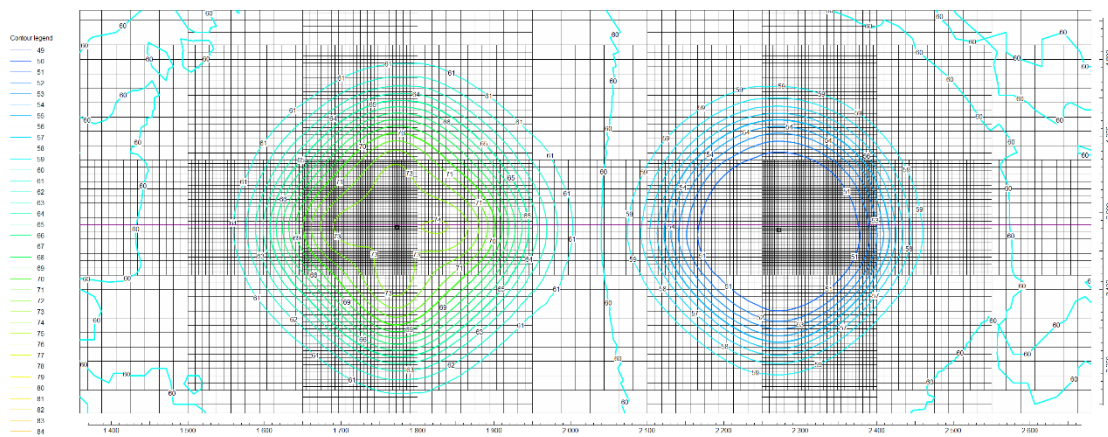


Figure 45 Period 2 Step 6

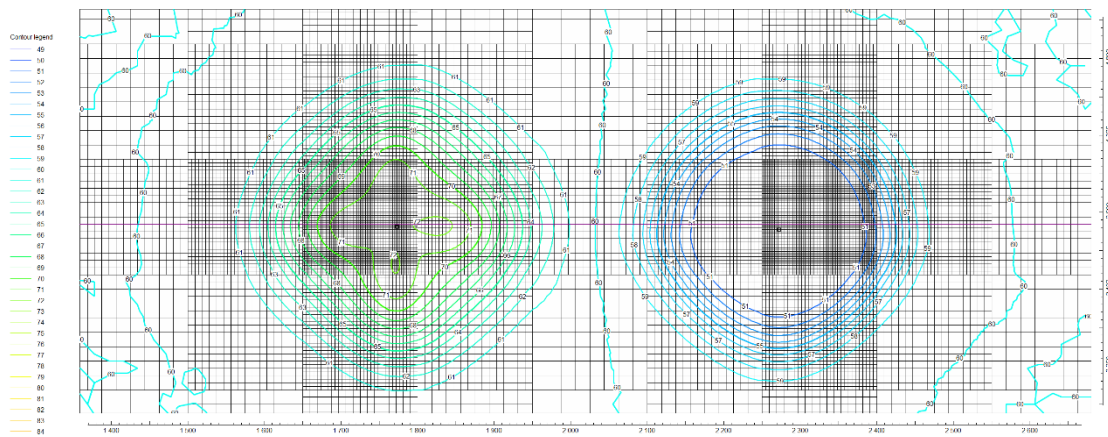


Figure 46 Period 2 Step 7

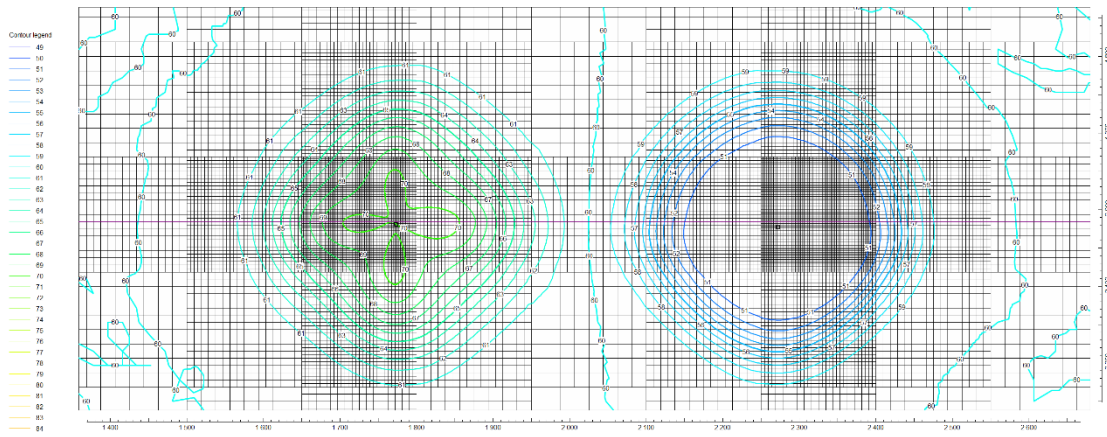


Figure 47 Period 2 Step 8

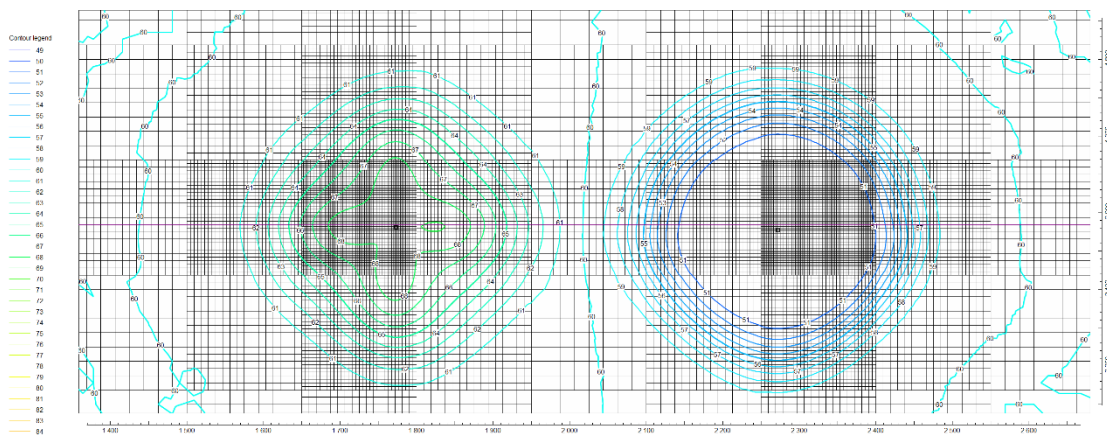


Figure 48 Period 2 Step 9

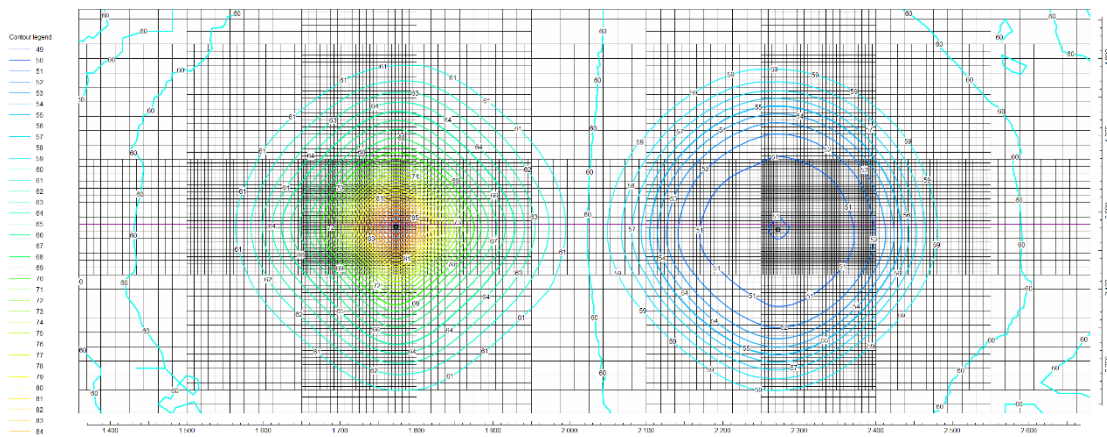


Figure 49 Period 2 Step 10



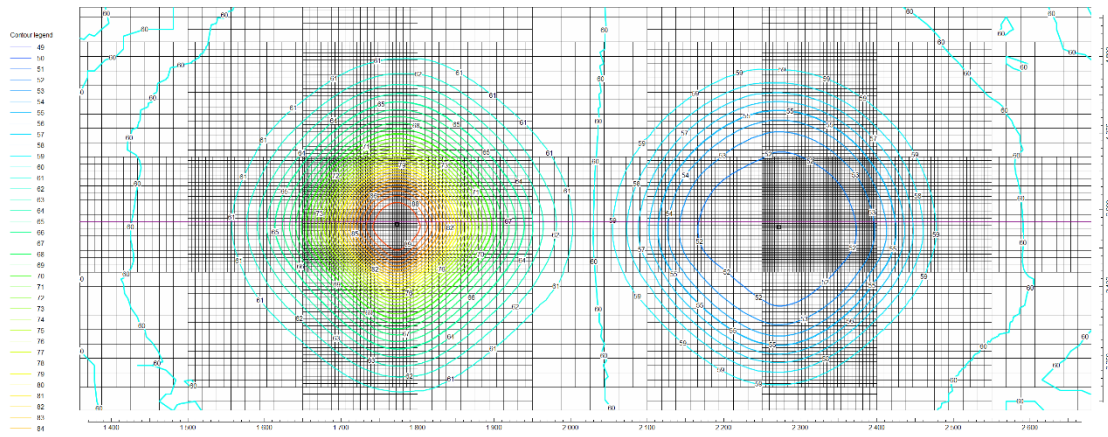


Figure 50 Period 3 Step 1

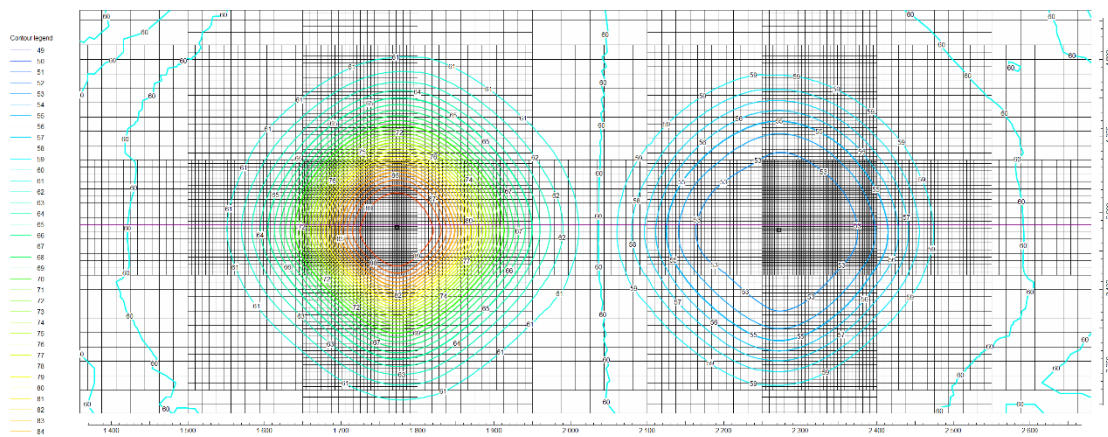


Figure 51 Period 3 Step 2

## List of Figures

Figure 1: The potential waste heat distribution in Vienna. (Loibl et al., 2017, p. 10).....	10
Figure 2 ATES-Mono and Doublet-System.....	11
Figure 3 Temperature profile of the Wells: Enzersdorf 17 and Himberg 1 (Geologische Bundesanstalt, 2015).....	13
Figure 4 Geological cross section profile from the GBA Database, Autor: Elster et al. ....	14
Figure 5 Depiction of the screen length, which represents the open part of the well in the aquifer. ....	16
Figure 6 Comparison of drilling-cost formulas from different literature sources. The conversion factor between \$ and € has been kept to the current conversion rate of 1:1. ....	19
Figure 7 Profile of the adjusted Drilling-Cost Formula.....	20
Figure 8 The initial layout of the modflow model created with ModelMuse. The smallest cells are next to the wells. The distance between the wells is set as 500m due to the calculated thermal radius (Rth) .....	22
Figure 9 Temperature Profile of the initial modflow setup (3500m <sup>3</sup> /day, 50m reservoir thickness and 50C cut-off temperature). The blue line represents the production and injection from the hot well, respectively the orange line is the temperature profile of the cold well.....	26
Figure 10 Recovery efficiency of the initial modflow setup (3500m <sup>3</sup> /day, 50m reservoir thickness and 50C cut-off temperature).....	26
Figure 11 Depicting the difference between the results of cumulative CF and NPV for case 1 and impact of the discounted DHN price.....	27
Figure 12 LCOH-Sensitivity Analysis created with the sensitivity package. LCOH is depicted in €/MWh, Energy in MWh, Capex & Opex in €.....	28
Figure 13 ModelMuse graphical interpretation of the concentrations/temperature from the top view, providing an insight for the result after 730 days.....	29
Figure 14 Temperature profile comparison between the different volumetric scenarios (case 1&5) of both hot and cold wells. 630k and 728k represent the value of total production in one production period (one year). Additional figure with a higher resolution for the Hot Wells can be found in the Appendix A Figure 26. ....	30
Figure 15 Recovery efficiency comparison of the different volumetric case scenario (case 1&4) results. 50m representing the reservoir thickness and 50° C the cut-off temperature. ....	30
Figure 16 Temperature comparison with constant reservoir thickness of 50m and production rate 3500m <sup>3</sup> /day. The cut-off temperatures set to 50° C and 40° C. ....	31
Figure 17 Recovery efficiency of all the simulated scenarios. The legend represents the production rate of 3.5k-4k m <sup>3</sup> /day, 40-50° C cut-off temperature and the reservoir thickness of 50-75m. ....	32
Figure 18 Shows the impact due to the variation in cut-off temperature, on the overall cumulative energy provided by the system and the effect on the LCOH outcome.....	33
Figure 19 LCOH comparison for all the cases shown in Table 5 and the impact of 10-year change.....	33
Figure 20 Cash-flow sensitivity analysis for the variables: CAPEX, OPEX, DHN-Price and the electricity Price. ....	35
Figure 21 NPV-Comparison between all the simulated cases. The legend represents the production rate of 3.5k-4k m <sup>3</sup> /day, 40-50° C cut-off temperature and the reservoir thickness of 50-75m. Additionally the base case scenario (case 1) with discounted DHN price has been added to the plot for analogy. ....	35
Figure 22 The impact of discounting the DHN-price and no research and development time. ....	36
Figure 23: Energy Flow Vienna 2022 (Magistratsabteilung 20, 2022, p. 37).....	45

---

Figure 24 Cross section from the GBA website, depicting the Vienna Basin (GBA MapViewer, 2017; Geologische Bundesanstalt, 2015).....	46
Figure 25 Cross section from the GBA website, depicting the Vienna Basin (GBA MapViewer, 2017; Geologische Bundesanstalt, 2015).....	46
Figure 26 Well temperature profile from Schewacht 1a (Geologische Bundesanstalt, 2015; GBA MapViewer, 2017).....	47
Figure 27 Temperature profile comparison between the hot wells of different volumetric scenarios.....	48
Figure 28 Close-up of the ModelMuse grid used for the simulation, depicting the Hot and the Cold wells. ....	48
Figure 29 Period 1 Step 1.....	49
Figure 30 Period 1 Step 2.....	49
Figure 31 Period 1 Step 3.....	49
Figure 32 Period 1 Step 4.....	50
Figure 33 Period 1 Step 5.....	50
Figure 34 Period 1 Step 6.....	50
Figure 35 Period 1 Step 7.....	51
Figure 36 Period 1 Step 8.....	51
Figure 37 Period 1 Step 9.....	51
Figure 38 Period 1 Step 10.....	52
Figure 39 Period 2 Step 1.....	52
Figure 40 Period 2 Step 2.....	52
Figure 41 Period 2 Step 3.....	53
Figure 42 Period 2 Step 3.....	53
Figure 43 Period 2 Step 4.....	53
Figure 44 Period 2 Step 5.....	54
Figure 45 Period 2 Step 6.....	54
Figure 46 Period 2 Step 7.....	54
Figure 47 Period 2 Step 8.....	55
Figure 48 Period 2 Step 9.....	55
Figure 49 Period 2 Step 10.....	55
Figure 50 Period 3 Step 1.....	56
Figure 51 Period 3 Step 2.....	56

## List of Tables

Table 1	Current known and upcoming HT-ATES Projects .....	12
Table 2	Input parameters for the technical assessment .....	17
Table 3	Inputs for the economical assessment .....	21
Table 4	Sensitivity inputs for the modflow model scenarios .....	29
Table 5	LCOH – All scenarios in comparison, being referred to as cases 1 to 8.....	34

# Nomenclature

$L$	Screen Length	m
$R_{th}$	Thermal Radius	m
$E$	Energy	MWh
$g$	Gravity Acceleration	$m^2/s$
$\alpha$	Dispersivity	m
$c_w$	Heat Capacity Water	$J/kg/K^\circ$
$c_a$	Heat Capacity Aquifer	$J/kg/K^\circ$
$P_{ates}$	ATES Power	MW
$P_{pump}$	Pump Power	W
$V$	Volume	$m^3$
$Q$	Production Rate	$m^3/day$
$\eta$	Pump Efficiency	%
$\theta$	Porosity	%
$D_{temp}$	Molecular Diffusion coefficient	$m^2/s$
$k_t$	Thermal Conductivity	$W/m/K^\circ$
$k$	Hydraulic Conductivity	m/s
$HP_{cost}$	Heat Pump Cost	€
$e_{price}$	Electricity Price	€/kwh
$\delta$	Density	$kg/m^3$
$h$	Well Depth	m
$n$	Number of wells	-
$Capex_{drilling}$	Drilling costs	€
$Capex_{s.f.}$	Surface facility costs	€



## Abbreviations

HT-ATES	High Temperature – Aquifer Thermal Energy Storage
LT-ATES	Low Temperature – Aquifer Thermal Energy Storage
LCOH	Levelized Cost of Heat
LCOE	Levelized Cost of Energy
NPV	Net Present Value
MF6	Modflow 6
COLD well	Cold well is also often referred to as the balancing well in literature, it is used for the reinjection of the used water.
HOT well	Hot wells are used for the injection of heated water and its later retrieval.
CAPEX	Capital Expenditures
OPEX	Operational Expenditures
UTES	Underground Thermal Energy Storage
ATES	Aquifer Thermal Energy Storage
ESP	Electrical submersible pump
DHN	District Heating Network
LT	Low Temperature
HT	High Temperature
MW	Mega Watt
MWth	Mega Watt thermal
kWh	Kilo Watt Hours